American Mineralogist, Volume 74, pages 113–131, 1989

Alkaline igneous rocks of Magnet Cove, Arkansas: Metasomatized ijolite xenoliths from Diamond Jo quarry

MARTA J. K. FLOHR, MALCOLM ROSS
959 National Center, U.S. Geological Survey, Reston, Virginia 22092, U.S.A.

ABSTRACT

Ijolite xenoliths occur in garnet-pseudoleucite syenite that forms part of the outer ring of the Magnet Cove alkaline ring-dike complex. Xenoliths were collected from the Diamond Jo quarry located in the southern part of the complex. The xenoliths contain abundant diopside and Ti-rich andradite garnets and have been extensively metasomatized. Garnet-pseudoleucite syenite and nepheline syenite are identified as possible sources of the volatile-rich fluids responsible for the metasomatism of the ijolite xenoliths. Residual, volatile-rich fluids from the ijolites may have also produced autometasomatic alteration before the ijolites were entrained as xenoliths in the garnet-pseudoleucite syenite. Nonisotropic hydrogarnet, formed during metasomatism, contains up to 3.5 wt% F. Aegirine, biotite, and melanite garnet, also formed during metasomatism, contain relatively high amounts of V and/or Ti, indicating that these elements were transported by the metasomatic fluids. Mineral compositions and geochemical data indicate that the ijolite xenoliths share many characteristics with the intrusive ijolites that form the inner rings of the Magnet Cove complex.

INTRODUCTION

The Magnet Cove complex is an alkaline ring-dike complex that crops out in an area of approximately 12 km^2 in Hot Spring County, Arkansas. The igneous rocks of the complex intrude deformed Paleozoic sedimentary rocks of the Ouachita Mountains. Biotite K-Ar and Rb-Sr ages obtained by Zartman (1977) indicate a Cretaceous age of 95–102 Ma for the complex. Fission-track ages (Eby, 1987) indicate two periods of igneous activity at Magnet Cove. The mean sphene age for the emplacement of the silicate rock units is 101.4 ± 1.0 Ma, whereas the carbonatite, which occurs in the core of the complex, was emplaced about 5 m.y. later, as indicated by a mean apatite age of 95.9 ± 0.4 Ma. Magnet Cove is one of several alkaline igneous intrusions in central Arkansas. Morris (1987) described this diverse suite of rocks and discussed possible petrologic relationships among them. One purpose of the current study of the igneous rocks from Magnet Cove is to elucidate the relationships among the various rock types and to compare the petrologic evolution of Magnet Cove to that of the other intrusions of the Arkansas alkaline province.

Metasomatism has played an important role in the petrogenetic history of these rocks. All of the samples from the Diamond Jo quarry examined thus far show extensive replacement of primary magmatic minerals by secondary phases. In this paper, which is the first of a series on the Magnet Cove complex, we describe both the primary and secondary mineral assemblages found in ijolite xenoliths from the garnet-pseudoleucite syenite that forms part of the outer syenite ring of the Magnet Cove complex. We then consider the petrogenetic relationships of the ijolite xenoliths to the garnet ijolite and biotite-garnet ijolite that form the inner rings of the complex.

GEOLOGY

The rocks of Magnet Cove are host to numerous mineral species, and much of the early literature about the complex deals with the minerals. The first detailed petrographic study and geologic map of Magnet Cove were made by Williams (1891). Erickson and Blade (1963) remapped the Magnet Cove complex and presented a detailed lithologic and geochemical study of the igneous rocks and the surrounding country rocks. A generalized geologic map of the complex based on their detailed map is given in Figure 1. Erickson and Blade (1963) concluded that phonolites and trachytes were intruded first, followed by jacupirangite and the syenites of the outer ring, then the inner-ring ijolites, and finally carbonatite, which is found in the core of the complex. Erickson and Blade (1963) proposed that the igneous rocks of the Magnet Cove complex are related by differentiation and fractional crystallization of a residual, volatile-enriched phonolite magma and that this magma was derived by fractional crystallization of an undersaturated olivine basalt magma.

Exposures of fresh rocks are scarce within the complex. However, the opening of the Diamond Jo quarry in the latter part of the 19th century to supply stone ballast for the Hot Springs Railroad exposed much fresh unweathered rock. This quarry, which is located in the southern part of the complex and within the outer syenite ring (Fig.

0003–004X/89/0102–0113$02.00

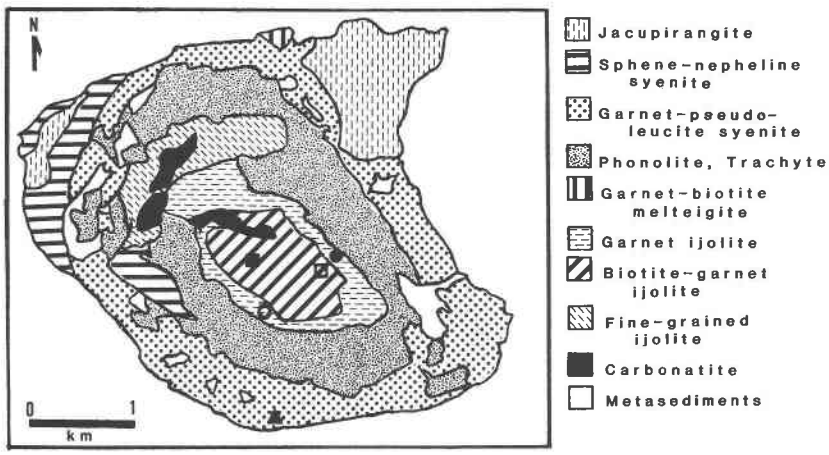

Fig. 1. Generalized geologic map of the Magnet Cove alkaline igneous complex, Hot Spring County, Arkansas, after Erickson and Blade (1963). The Diamond Jo quarry (solid triangle) is the sampling site of the ijolite xenoliths described in this paper. The open and solid circles mark, respectively, the approximate sampling locations of garnet ijolites 99423/7 and 85-13B-RSS; the open and solid squares mark, respectively, the approximate sampling locations of biotite-garnet ijolites 99423/6 and 85-16-RSS.

1), was mapped in detail by Owens and Howard (1989), and a simplified version of part of their map is shown in Figure 2. The two rock types exposed on the walls of the quarry are nepheline syenite (originally mapped by Erickson and Blade, 1963, as nepheline syenite pegmatite) and garnet-pseudoleucite syenite. The contact between these two rock types is relatively sharp. The garnet-pseudoleucite syenite contains abundant xenoliths of ijolite, ranging from a few millimeters to 3 m in diameter. Xenoliths of Stanley shale, now metamorphosed to hornfels, are also found within the garnet-pseudoleucite syenite. Preliminary petrographic and electron-microprobe data from the Diamond Jo syenites and ijolite xenoliths were given by Ross (1984) and Flohr and Ross (1985a, 1985b).

Methods of analysis

Mineral compositions were obtained by using an automated ARL-SEMQ[1] electron microprobe operating at 15 kV with a beam current of 0.1 μA using either an 8- or 9-spectrometer configuration. Correction procedures of Bence and Albee (1968) and alpha-factor modifications of Albee and Ray (1970) were used. During analysis of cancrinite and natrolite, the electron beam was rastered over an area of 4 μm^2 in order to minimize loss of Na due to mobilization. Data collection procedures were outlined by McGee (1983, 1985), and backgrounds were calculated using an interpolation routine described by M. Mangan and J. J. McGee (written comm., 1985). A variety of natural and synthetic materials were used as standards. Traverses of clinopyroxenes were obtained using an ARL-EMX 3-channel electron microprobe. X-ray single-crystal and powder-diffraction data were obtained on selected crystals. Whole-rock analyses were obtained on three ijolite xenoliths (1-166B, 1-143, and 5-DJ7) and two inner-ring ijolites (85-13B-RSS and 85-16-RSS) using analytical methods described by Baedecker (1987).

[1] Any use of trade names in this report is for descriptive purposes only and does not imply endorsement by the U.S. Geological Survey.

Whole-rock compositions of Magnet Cove ijolites

Whole-rock major-, minor-, and trace-element compositions of ijolite xenoliths 5-DJ7, 1-166, and 1-143 (Tables 1, 2) reflect the modal diversity of the ijolite xenolith suite (Table 3). Included in Tables 1 and 2 are analyses of a garnet ijolite and a biotite-garnet ijolite from the inner-ring ijolite for preliminary comparison with the ijolite xenoliths. Major- and minor-element compositions of several additional ijolites from the inner ring are reported by Erickson and Blade (1963, their Table 17). Descriptions by Erickson and Blade indicate that these samples are similar to the inner-ring ijolites included in this study. Overall, the inner-ring ijolites are slightly more magnesian and contain significantly less F and CO_2 than the ijolite xenoliths.

Of the three analyzed ijolite xenoliths, 1-143 contains the highest abundance of clinopyroxene plus garnet and is enriched in Ti, Fe, and Ca and depleted in Si, Al, and Na compared with samples 1-166 and 5-DJ7. Xenolith 1-143 is also enriched in V, Y, and Zr, compared to samples 5-DJ7 and 1-166. These are trace elements commonly found in notable concentrations in garnets from alkaline igneous rocks (e.g., Deer et al., 1982 and this study). Schnetzler and Philpotts (1970) also reported that garnet has high distribution coefficients for the heavy rare-earth elements (HREEs) compared to other common rock-forming minerals. In the ijolite xenoliths, as the abundance of garnet increases from 10% in 5-DJ7 to an average of 37% in 1-143, the HREE concentration increases (Fig. 3). Garnet ijolite 85-13B-RSS from the inner-ring ijolite has REE concentrations (Table 2) and a REE pattern similar to those of the ijolite xenoliths, whereas biotite-garnet ijolite 85-16-RSS has a much more fractionated REE pattern. Ijolites from the Fen complex, Norway (Mitchell and Brunfelt, 1975), Seabrook Lake, Ontario

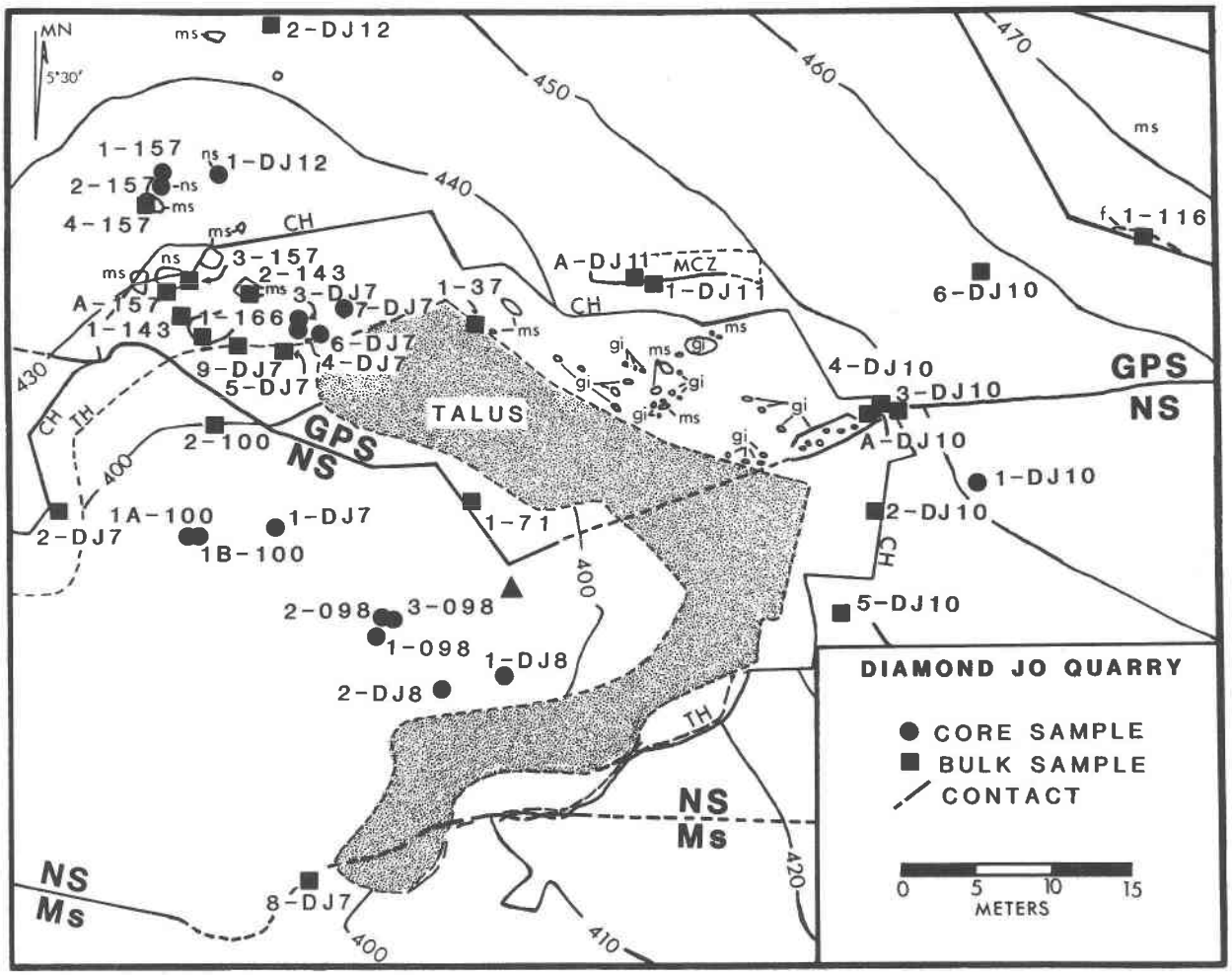

Fig. 2. Geologic map of the Diamond Jo quarry, Magnet Cove complex, after Owens and Howard (1989) indicating locations of all core and bulk samples of ijolite xenoliths and syenites collected. Samples 84-1-RSS-A and B are grab samples collected from the talus slope. Contour interval is 10 ft (3.048 m). NS, nepheline syenite; GPS, garnet-pseudoleucite syenite; Ms, Stanley shale; f, fenite; ns, nepheline syenite xenoliths (?); gi, garnet ijolite xenoliths; ms, metamorphosed Stanley shale xenoliths; MCZ, mafic clot zone; CH and TH, crest and toe respectively, of highwall. The solid triangle marks the location of survey station DJ8 at lat 34°26′17″N and long 92°51′45″W.

(Cullers and Medaris, 1977) and Oka, Quebec (Eby, 1975), have relatively fractionated REE patterns that are similar to the pattern of the biotite-garnet ijolite from Magnet Cove. Mitchell and Brunfelt (1975) noted that with increasing abundance of garnet, the REE patterns of the ijolites from the Fen complex became progressively flatter, i.e., the light REEs (LREEs) are less enriched relative to the HREEs. Abundance of garnet in the ijolites from Magnet Cove thus exercises significant control over the REE patterns of these rocks.

Despite the range of trace-element compositions in the three analyzed ijolite xenoliths, these rocks are generally typical of mafic alkaline rocks (e.g., Gerasimovsky et al., 1968; Gerasimovsky, 1974; Sage, 1987). Relatively high concentrations of Pb in xenoliths 5-DJ7 and 1-166 and low concentrations of Th, Nb, and Ta, and low Th/U in all three xenoliths (Table 2) are notable exceptions. Ijolites from the inner ring contain significantly less Pb than the ijolite xenoliths. Garnet ijolite 85-13B-RSS shares some characteristics with the ijolite xenoliths, but is depleted in Ba and Rb relative to them, unlike garnet-biotite ijolite 85-16-RSS, which contains significantly more Ba, and also Sr, but has a similar amount of Rb. Additional data are needed to fully compare the geochemistry of the ijolite xenoliths and inner-ring ijolites.

Petrography and mineral compositions of the ijolite xenoliths

Nine samples of ijolite xenoliths were collected from the Diamond Jo quarry; six are bulk samples (1-143A, 1-143B, 1-166B, 5-DJ7, 84-1-RSS-A, and 84-1-RSS-B) and three are drill-core samples having diameters of 2.54

TABLE 1. Whole-rock major- and minor-element compositions (in wt%) of ijolites from the Magnet Cove igneous complex, Arkansas

	Ijolite xenoliths, Diamond Jo quarry			Inner-ring ijolites	
Sample:	5-DJ7	1-166	1-143	85-13-RSS	85-16-RSS
SiO_2	40.5	37.5	35.4	41.1	34.2
TiO_2	1.6	2.3	5.9	2.40	3.61
Al_2O_3	19.1	17.9	12.0	14.2	16.1
Fe_2O_3	5.3	5.3	8.9	5.56*	8.13*
FeO	3.3	3.9	3.8	3.27	2.85
MnO	0.21	0.19	0.28	0.40	0.30
MgO	3.0	3.8	3.3	5.13	7.16
CaO	13.1	14.6	19.5	16.2	14.0
Na_2O	7.9	7.3	4.3	6.03	3.40
K_2O	3.6	2.7	1.7	3.20	2.34
P_2O_5	0.64	0.80	0.72	1.08	1.22
H_2O	1.40	1.78	1.92	0.46	5.99
CO_2	0.74	2.0	0.98	0.28	0.24
Cl	0.055	0.140	0.009	0.02	<0.01
F	0.45	0.30	0.24	0.07	0.04
S	0.23	0.26	0.39	0.21	0.42
Sum	101.1	100.8	99.34	99.61	100.0

Note: Major oxides, excluding FeO, determined by ICP-AES (inductively coupled plasma–atomic emission spectrometry) by M. Kavulak, J. Marinenko, and R. Rait in the ijolite xenoliths, and by X-ray fluorescence by J. Taggart, A. J. Bartel, and D. Siems in garnet ijolite 85-13B-RSS and biotite-garnet ijolite 85-16-RSS. FeO, H_2O, CO_2, S, F, and Cl determined by various techniques by E. Brandt, J. H. Christie, J. Sharkey, L. Jackson, M. Kavulak, J. Marinenko, and N. Rait.

* Fe_2O_3 calculated from total Fe obtained as Fe_2O_3 and reported FeO.

TABLE 2. Whole-rock minor- and trace-element compositions (in ppm) of ijolites from the Magnet Cove igneous complex, Arkansas

	Ijolite xenoliths, Diamond Jo quarry			Inner-ring ijolites	
Sample:	5-DJ7	1-166	1-143	85-13B-RSS	85-16-RSS
La	21.8	15.8	25.5	24.5	92.2
Ce	28.8	20.5	36	38.6	93
Nd	10.8	11.0	21.6	19.7	26.0
Sm	2.74	3.61	10.29	4.6	6.8
Eu	0.94	1.34	4.69	1.59	2.46
Tb	0.527	0.98	5.50	0.94	1.31
Yb	3.20	6.51	47.7	5.59	2.03
Lu	0.478	0.91	6.01	0.80	0.204
Ba	778	440	617	25	2040
Rb	171	117	149	51	119
Sr	874	695	843	678	1120
Nb	32	12	54	21	224
Ta	1.21	0.80	3.05	1.73	3.78
Zr	439	572	1720	714	42
Hf	5.05	7.93	31.9	13.3	0.69
Y	28	52	394	37	26
Th	0.97	0.19	1.57	1.77	1.06
U	1.09	0.72	2.05	1.33	5.99
Sc	0.31	0.74	6.30	4.71	2.31
V	980	970	1300	810	700
Cr	4.4	3.6	3.4	7.6	3.6
Co	4.68	13.8	16.0	18.9	36.2
Ni	<50	<50	<70	<70	<80
Cu	12	11	5.0	18	26
Zn	52.8	47	153	55	82
Sb	25.9	3.20	10.2	0.155	0.19
Cs	3.88	2.78	3.18	0.33	1.36
Pb	94	15	47	<5	<5
Zr/Hf	86	72	54	54	61
Nb/Ta	26	15	18	12	59
Th/U	0.89	0.26	0.77	1.3	0.18
Rb/Ba	0.22	0.27	0.24	0.075	0.11

Note: Ba, Rb, Sr, Nb, Y, and Zr determined by energy-dispersive X-ray fluorescence spectroscopy by J. Evans. V, Cu, and Pb determined by atomic absorption by M. Doughton. All other elements determined by instrumental neutron-activation analysis by J. Mee.

cm and lengths ranging from 7.01 to 9.75 cm (4-DJ7, 3-DJ7, and 6-DJ7). Sample locations are shown in Figure 2. Samples 84-1-RSS-A and -B are grab samples collected from the talus slope.

According to the modal classification of alkaline rocks presented by Sørensen (1974), 4-DJ7, 1-166B, 1-143A, and 3-DJ7 are melteigites, and the rest of the samples are ijolites (Table 3). By definition, ijolites and melteigites contain between 10% and 70% nepheline (Sørensen, 1974). Two of the ijolite xenoliths do not contain any nepheline (Table 3) owing to replacement by cancrinite and natrolite. For the sake of simplicity and to be consistent with the terminology used by Erickson and Blade (1963), we will collectively refer to the suite of samples as ijolites. Photomicrographs (Figs. 4a–4d) illustrate the varied modes and textures found in the ijolite xenoliths and inner-ring ijolites.

Despite the variable modes found in the ijolite xenoliths, mineral compositions indicate that these rocks form a coherent group. The xenoliths experienced varying degrees of metasomatism resulting in the textural and, to some extent, the modal variations seen among samples. Metasomatism is also responsible for some of the compositional differences found in the minerals, both within individual samples and among different samples.

Primary igneous minerals are distinguished from later-formed metasomatic minerals by using textural criteria. (Metasomatic minerals are here defined as those minerals formed as the result of reaction between earlier-crystallized primary igneous minerals and volatile-rich fluids. These fluids may be residual fluids from the ijolites themselves or be derived from external sources.) Diopsidic clinopyroxene, nepheline, and garnets of Groups I and IIA (defined in the section entitled Garnets) are identified as the primary rock-forming minerals. Primary accessory minerals, which occur as inclusions within diopside, nepheline, and/or garnets of Groups I and IIA, are perovskite, equant apatite, and magnetite. Progressive replacement of nepheline by minerals formed during metasomatism is observed. Total replacement of nepheline occurs in some of the ijolite xenoliths (Table 3). Replacement of nepheline commences by the formation of cancrinite along fractures within the nepheline. In more advanced stages of replacement, intergrown grains of cancrinite and, usually, subordinate amounts of natrolite and calcite are found, and only small patches of nepheline remain. Magmatic textures are preserved in ijolite xenoliths 6-DJ7 and 5-DJ7 that contain only partially replaced nepheline. In xenolith 6-DJ7, laths of diopside are ophitically to subophitically enclosed by nepheline, and 5-DJ7

has an intergranular to subophitic texture. As replacement of nepheline by hydrous silicates and calcite progresses, diopside is replaced by biotite. Biotite is never observed replacing diopside where the latter is in contact with unaltered nepheline. Similarly, low-Ti garnets (Groups III and IV) never occur as overgrowths or rims on the high-Ti schorlomite or melanite garnets (Groups I or IIA) where these primary garnets are in contact with diopside or nepheline; rather garnets of Groups III and IV formed by reaction between primary garnet and metasomatic fluid. The melanite garnets of Group II are somewhat problematic in their petrogenesis, as they rim primary Group I schorlomite garnets and also form subhedral grains intergrown with metasomatically formed phases. Garnets of Group II may represent a transitional stage of garnet crystallization. A second generation of apatite forms acicular to tabular grains within masses of cancrinite, natrolite, and calcite. Aegirine-augite and a second generation of magnetite are associated with metasomatic silicates and calcite and appear to be contemporaneous with these minerals.

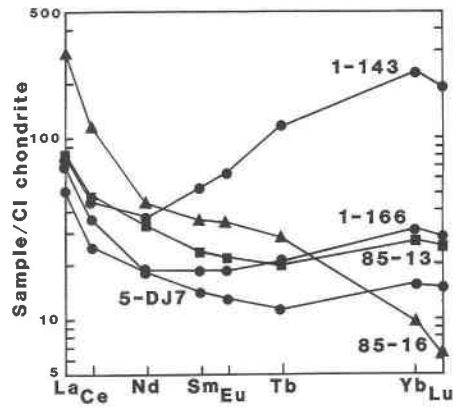

Fig. 3. Chondrite-normalized rare-earth-element patterns for ijolite xenoliths (1-143, 1-166, and 5-DJ7) and inner-ring ijolites (garnet ijolite 85-13B-RSS and biotite-garnet ijolite 85-16-RSS).

Clinopyroxenes

Primary clinopyroxenes occur in all the ijolite xenoliths. In all the samples except 6-DJ7, these pyroxenes are subhedral to euhedral, sector zoned, pleochroic, and partially replaced by biotite. Fine, oscillatory zoning is superimposed on the sector zoning in some grains. Most of these clinopyroxenes are 2–5 mm long, although grains up to about 2 cm long are found in the coarsest sample, 4-DJ7 (Fig. 4b). (The nomenclature used in describing pyroxenes follows that recommended by the International Mineralogic Association Subcommittee on Pyroxenes, Morimoto, 1988.) The sector-zoned clinopyroxenes are subsilicic aluminian ferrian diopsides (Table 4, nos. 1–4). The overall compositional ranges are as follows: $Mg/(Mg + Fe^{2+} + Fe^{3+}) = 0.447$ to 0.619, $Al_2O_3 = 7.15$ to 12.1 wt%, $TiO_2 = 1.45$ to 3.92 wt%, $Na_2O = 0.45$ to 0.70 wt%, and MnO = 0.17 to 0.45 wt%. CaO is uniformly high, ranging from 22.7 to 24.4 wt%. Pleochroic light- to medium-lilac or pink sectors are consistently higher in Al, Ti, and total Fe and lower in Mg than pleochroic light- to medium-green sectors. No differences in the concentrations of Ca, Mn, and Na were detected between sectors. A traverse of one sector-zoned diopside, 2.6 mm across, from sample 84-1-RSS-A1 (subhedral grain shown in the lower left quadrant of Fig. 4a) was made with the microprobe. Count data for Al, Ti, and Si were collected at 15-μm intervals. The data indicate that the compositional boundary between sectors is abrupt, with Ti and Al significantly decreasing in concentration from the outer to the inner sectors and Si slightly increasing. Within

Table 3. Modes (in vol%) of ijolites from the Magnet Cove igneous complex, Arkansas

	Ijolite xenoliths from Diamond Jo quarry									Inner-ring ijolites	
Sample:	4-DJ7-1,2	1-166B-4	5-DJ7-1,5	6-DJ7-1,3	84-1-RSS-A1	84-1-RSS-B2	1-143A-1,2	1-143B-3	3-DJ7-1,2	99423/7†	99423/6†
Clinopyroxene	55.1	37.8	33.3	28.7	19.5	19.4	16.6	16.5	10.7	25.8	0
Garnet	2.8	17.4	10.4	11.2	26.9	19.7	39.5	34.4	43.9	9.0	16.2
Biotite	16.4	15.7	8.2	8.8	9.3	8.4	11.6	12.6	21.5	2.7	11.8
Sphene	2.8	0.6	0.8	5.0	1.8	1.5	1.6	0.8	2.8	0	0
Apatite	3.9	3.4	1.3	2.9	3.4	2.1	1.2	1.1	2.3	0.9	0
Magnetite	0.2	0	0.2	0.4	trace	trace	trace	0	0.1	2.3	7.1
Perovskite	0.6	0	0	0.8	0	0	0.3	0	0	5.4	1.9
Nepheline	0	0.6	28.2	21.9	0.5	11.4	0.3	0	0.1	52.4*	54.4‡
Cancrinite	13.4	5.4	13.7	19.0	16.7	26.3	11.4	20.8	0.7	0	0.4
Natrolite	0.2	15.5	2.9	0	16.0	9.5	15.0	11.7	11.7	0	0
Carbonate	4.2	2.6	0.5	0.5	5.0	1.3	1.8	1.9	5.7	0.2	4.2
Sulfide	0.2	1.0	0.3	0.4	0.8	0.2	0.4	trace	0.1	0.8	3.5
Other	0.1	0	0.1	0.4	0	0.2	0.2	0.2	0.4	0.4	0.4
	99.9	100	99.9	100	99.9	99.9	99.9	100	100	99.9	99.9
No. points	985	907	957	979	968	1007	975	931	908	1030	944

† Thin sections were obtained from the F. C. Calkins collection of 1918, curated by the National Museum, Washington, D.C. Sample 99423/7 is a garnet ijolite and sample 99423/6 is a biotite-garnet ijolite.

* Sum of altered (3.2%) and unaltered (49.2%) nepheline.

‡ Sum of altered (50.1%) and unaltered (4.3%) nepheline.

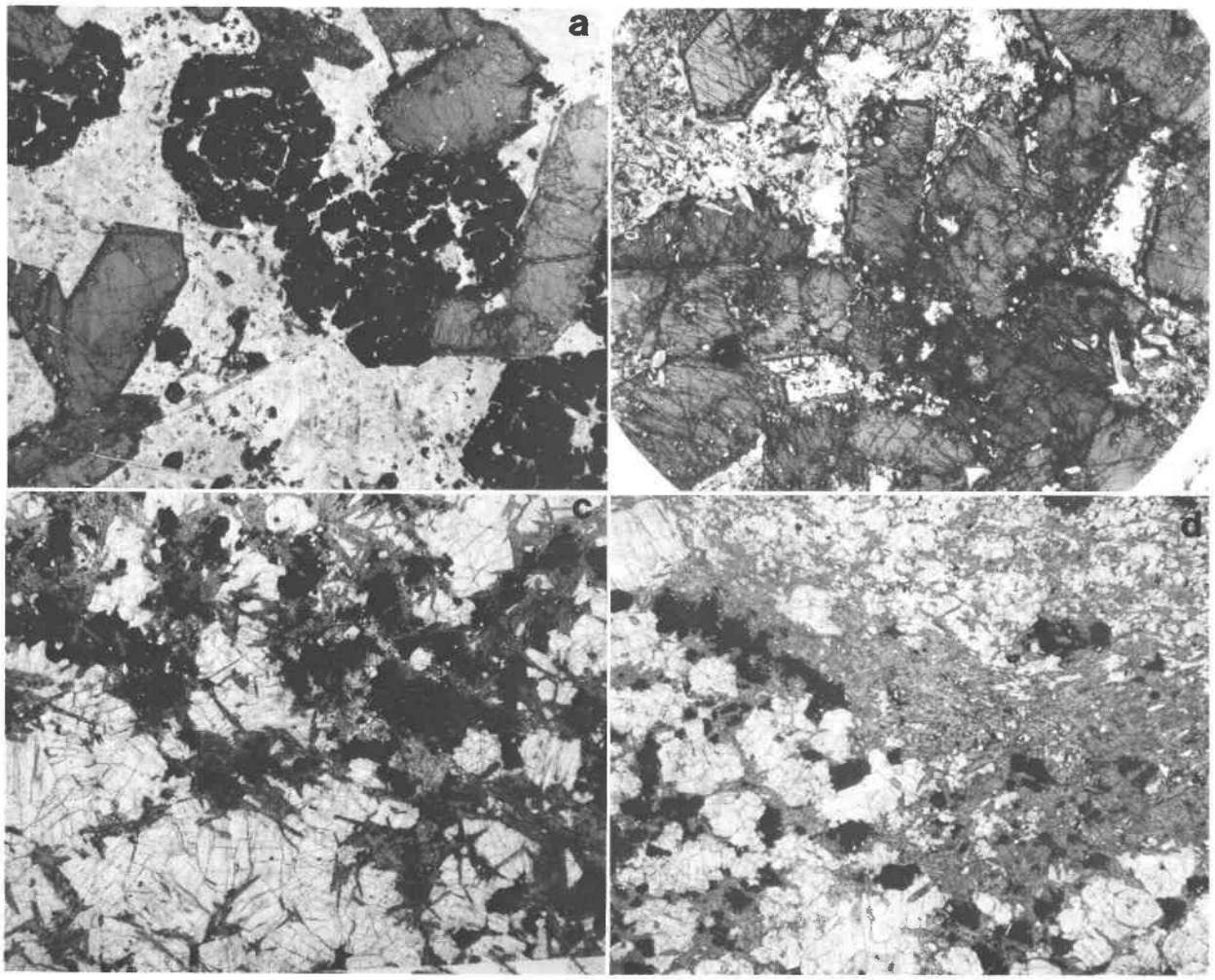

Fig. 4. Photomicrographs of thin sections of ijolites taken in plane-polarized light to illustrate varied modes and textures. Field of view is 2.1 cm across in all photomicrographs. Xenoliths from Diamond Jo quarry are shown in (a) and (b). (**a**) Sample 84-1-RSS-A1: euhedral to subhedral "atoll"-structured schorlomite garnets (black) with euhedral, tabular, sector-zoned clinopyroxenes marginally replaced by biotite in a light-colored groundmass of cancrinite, natrolite, and calcite, with minor melanite garnet (dark) and acicular apatite (lower-left quadrant). (**b**) Sample 4-DJ7-2: clinopyroxene (abundant tabular, subhedral to euhedral gray crystals) in a light-colored groundmass of cancrinite, calcite, and euhedral apatite (especially abundant in lower right, near edge of section). Inner-ring ijolites are shown in (c) and (d). (**c**) Garnet ijolite 99423/7: laths of clinopyroxene are interstitial to and included in equant (white) nepheline. Black areas are magnetite replacing perovskite. Clinopyroxene, together with minor garnet and biotite, is also intergrown with the oxides forming clots or aggregates. (**d**) Garnet ijolite 85-13B-RSS: laths of diopside (gray) are interstitial to nepheline (white) in lower left and upper right and form an aggregate in central part of the photograph. Large black grains are garnet; smaller black grains are garnet and sulfide.

both sectors, Ti and Al show minor fluctuations in concentration.

In 6-DJ7, the finest-grained ijolite xenolith, primary clinopyroxenes form laths up to 2 mm long, some of which are twinned. Clinopyroxenes from 6-DJ7 are also subsilicic aluminian ferrian diopsides (Table 4, no. 5) but are, on the average, more magnesian than the sector-zoned diopsides from the other ijolite xenoliths, with Mg/(Mg + Fe^{2+} + Fe^{3+}) = 0.555 to 0.729. These diopsides are also slightly less aluminous than the sector-zoned diopsides and have Al_2O_3 ranging from 5.61 to 9.07 wt%. They are continuously zoned. Some laths are rimmed by aegirine-augite and are not partially replaced by biotite as are the diopsides from the other xenoliths.

Pyroxenes, which are the products of metasomatism, are found in several of the ijolite xenoliths. In 5-DJ7 (Table 4, no. 6) and 4-DJ7, pale- to medium-green pleochroic aegirine-augite is intergrown with and is apparently replacing bioite, which itself has replaced primary diopside. Aegirine-augite having a similar composition occurs as single grains or aggregates in the groundmass of 3-DJ7. Ti-rich aegirine (Table 4, no. 7) in 4-DJ7 occurs

TABLE 4. Clinopyroxenes from the ijolite xenoliths, Diamond Jo quarry

Sample:	84-1-RSS-B2		5-DJ7-2A		6-DJ7-1	5-DJ7-2A	4-DJ7-2
	1	2	3	4	5	6	7
				Weight percent			
SiO_2	39.9	41.8	41.5	43.9	45.5	50.9	51.8
TiO_2	3.42	2.51	2.30	1.85	2.38	0.18	3.22
Al_2O_3	11.2	9.78	8.80	7.77	6.21	0.89	1.52
V_2O_3	nd	nd	0.19	0.20	0.12	0.09	0.56
Fe_2O_3*	8.37	8.45	10.5	8.23	7.52	9.32	26.6
FeO*	4.39	4.20	4.06	5.27	5.11	8.35	1.20
MnO	0.22	0.23	0.30	0.38	0.40	0.46	0.17
MgO	8.11	8.81	8.25	9.11	9.99	7.32	0.60
CaO	22.9	23.2	23.2	23.1	22.7	18.5	0.70
Na_2O	0.52	0.51	0.59	0.58	0.87	3.38	13.2
Sum	99.03	99.49	99.69	100.4	100.8	99.39	99.57
				Cations			
Si	1.543	1.604	1.603	1.673	1.719	1.961	1.977
Al	0.457	0.396	0.397	0.327	0.279	0.039	0.023
	2.000	2.000	2.000	2.000	1.995	2.000	2.000
Al	0.053	0.046	0.003	0.022	0	0.001	0.045
Ti	0.099	0.072	0.067	0.053	0.068	0.005	0.092
V	0	0	0.006	0.006	0.004	0.003	0.017
Fe^{3+}	0.244	0.244	0.305	0.236	0.214	0.270	0.764
Fe^{2+}	0.142	0.135	0.131	0.168	0.161	0.269	0.038
Mn	0	0	0.010	0	0	0.015	0.005
Mg	0.462	0.503	0.475	0.515	0.553	0.421	0.034
	1.000	1.000	0.997	1.000	1.000	0.984	0.995
Mn	0.007	0.007	0	0.012	0.013	0	0
Mg	0.005	0.001	0	0.002	0.010	0	0
Ca	0.949	0.954	0.959	0.943	0.918	0.763	0.029
Na	0.039	0.038	0.044	0.043	0.064	0.253	0.976
	1.000	1.000	1.003	1.000	1.005	1.016	1.005
No. pts. averaged	5	8	6	7	4	7	5

Note: nd = not detected. Column headings as follows: 1, 2—Sector-zoned grain with no. 1 from sector richer in Al and Ti than sector characterized in no. 2; 3, 4—Sector-zoned grain with no. 3 from sector richer in Al and Ti than sector characterized in no. 4; 5—Lath enclosed within nepheline; 6—Secondary aegirine-augite intergrown with and rimming biotite; 7—Fibrous aegirine intergrown with magnetite, garnet, and calcite in groundmass.
* Fe^{3+} and Fe^{2+} calculated by assuming ideal stoichiometry of 4 cations per 6 oxygens.

as fibrous masses intergrown with pale-pink garnet, calcite, cancrinite, apatite, and titanomagnetite and also forms clusters of fibers in the cores of apatite. It is the only pyroxene analyzed containing significant amounts of V, 0.47 to 1.04 wt% V_2O_3.

In the primary clinopyroxenes, Al primarily substitutes for Si in the tetrahedral site, while Ti enters the octahedral site, resulting in the positive correlation between Al and Ti seen in Figure 5a. Clinopyroxenes from 6-DJ7 contain amounts of Ti comparable with the other xenolith pyroxenes, but generally have slightly lower amounts of Al. Both Al (Fig. 5b) and Ti increase with decreasing $Mg/(Mg + Fe^{2+} + Fe^{3+})$ in the primary clinopyroxenes. Diopsides from 5-DJ7 cluster at the low Al and Ti end of the main group of pyroxenes and also are at the low end of the range of $Mg/(Mg + Fe^{2+} + Fe^{3+})$ for the group.

Garnets

Garnets are classified into four groups (I to IV) based on compositions. These groups indicate the crystallization sequence for the garnets. Representative microprobe analyses are presented in Tables 5 and 6, and data are plotted in Figures 6 and 7. A detailed explanation of the methods used to calculate the formulae of all the garnets (Tables 5, 6) is given in Appendix 1. The data plotted in Figure 6 represent the complete data set (Groups I–IV), whereas the data plotted in Figure 7 are only those of the F-bearing garnets of Group III. Andradite garnets containing >15 wt% TiO_2 are classified as schorlomites, and those containing <15 wt%, as melanites, following the criterion of Deer et al. (1982).

Group I garnets are dark-red to black schorlomites containing 15.5–18.2 wt% TiO_2 and occur in all samples except 5-DJ7. Group I garnets have morphologies ranging from poikilitic with an "atoll"' structure (Fig. 4a) to anhedral to subhedral grains up to 7 mm across. Compositions are uniform among samples, and zoning within single crystals is slight. In contrast, garnets in 5-DJ7 are melanites containing 8–10 wt% TiO_2. Compositionally these garnets belong to Group II (melanites); however, because they are morphologically different from other Group II garnets, they are differentiated as Group IIA. Garnets of Group IIA form anhedral to subhedral grains up to 5 mm across and commonly contain abundant apatite inclusions.

Melanite garnets (Group II) have a much wider compositional range than garnets of Group I. They form light-red to brown rims, up to 50 μm wide, on some of the

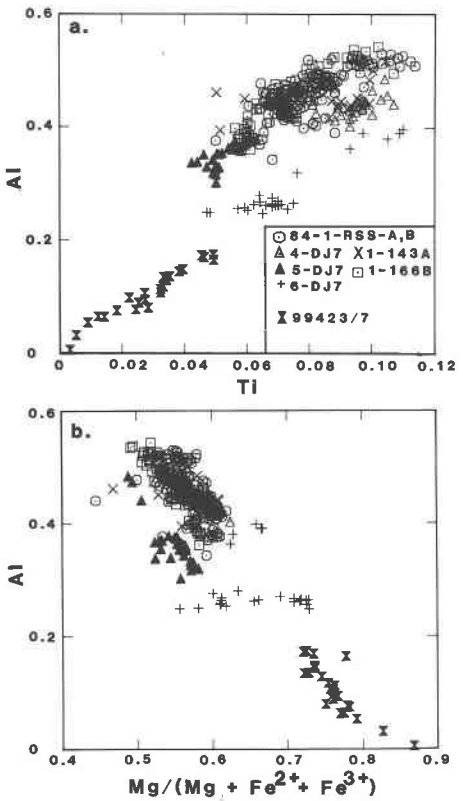

Fig. 5. Variation of total Al with (a) Ti and (b) Mg/(Mg + Fe^{2+} + Fe^{3+}) in primary clinopyroxenes (cations per 6 oxygens) from ijolite xenoliths and garnet ijolite 99423/7. Symbol key for both plots is given in (a).

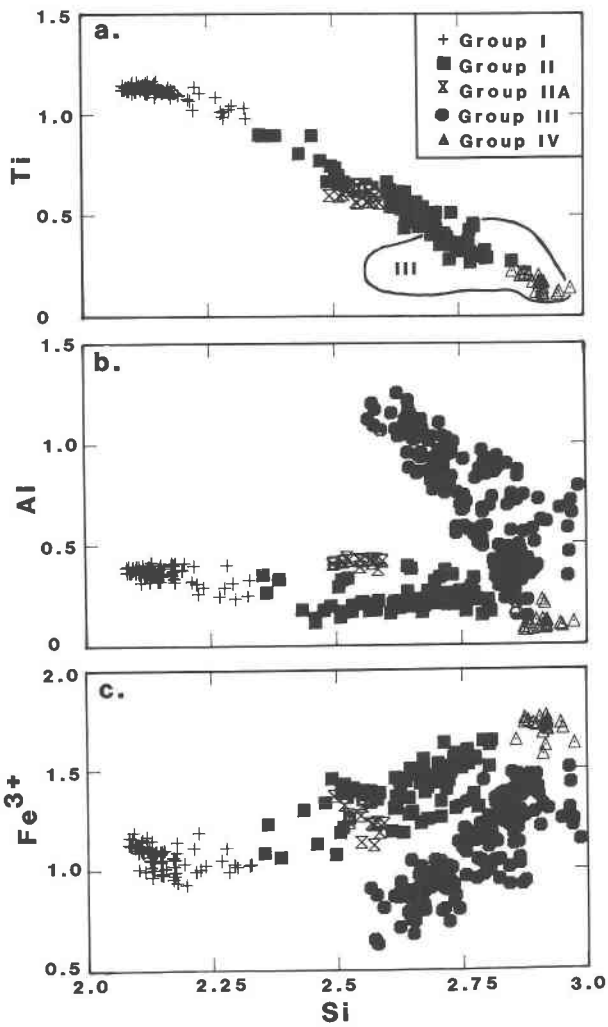

Fig. 6. Variation of (a) Ti, (b) Al, and (c) Fe^{3+} with Si in garnets (cations per 12 oxygens) from ijolite xenoliths. In (a), Group III garnets do not lie along the trend defined by Groups I, II, IIA, and IV and hence are not plotted so as not to obscure this trend; only the field where Group III garnets would plot is indicated. Groups are defined in the text. Symbol key for all three plots is given in (a).

schorlomites and occur as small subhedral grains in the groundmass. Melanites contain slightly more Mn and Ca and less Al, Mg, and Fe^{2+} on the average than do the schorlomites.

Group III garnets (Table 6) are the most unusual because they contain as much as 3.56 wt% F. They form colorless to pale-yellow, slightly birefringent overgrowths, which range in thickness from a few micrometers to about 40 μm, on melanites and schorlomites. These overgrowths are zoned and compositionally range from andradites to grossulars (grandite series); we refer to them as fluoro-hydrograndites. Initial microprobe analyses yielded low oxide sums even after analyzing for F, suggesting the presence of a hydrogarnet component. The presence of OH was verified by Anne Hofmeister (Geophysical Laboratory), who obtained a mid-IR spectrum of a garnet grain from 1-166B. This grain was approximately 30 μm across, was composed of nearly all colorless garnet with two small red areas (probably melanite garnet), and appeared optically to be very similar to the colorless overgrowth on a melanite garnet from 1-166B (Fig. 8). The IR spectrum represents an average of the entire crystal, including the small amounts of red melanite garnet. The amount of OH (calculated as water) indicated by the IR spectrum is 0.1–0.5 wt% (A. Hofmeister, written comm., 1986), less than that indicated by the low sums of the microprobe analyses of other colorless garnets (Table 6). Microprobe data show a strong negative correlation between oxide sums and F contents of the fluoro-hydrograndites, suggesting that the OH content increases as the F content increases. Given that the IR spectrum represents an average of the analyzed grain and that microprobe data indicate that the fluoro-hydrograndites are significantly zoned with respect to F (Table 6, nos. 4, 5) and probably OH, the low amount of H_2O indicated by the IR data is not totally unreasonable or inconsistent with the microprobe data. The grain from which the IR spectrum was obtained was unfortunately lost before it could be analyzed by microprobe.

The garnets of Group IV are low-Ti melanites and con-

tain little or no F. These garnets are the most Fe-rich and Al-poor garnets found in the ijolites and occur both as rims on fluoro-hydrograndite overgrowths and as pale-pink skeletal grains in the groundmass of 4-DJ7 (Table 5, no. 7). Enrichment of V occurs in the Group IV garnets; over 1 wt% V_2O_3 was found in some overgrowths (Table 5, no. 8).

A strong negative correlation exists between Ti and Si in the Group II, IIA, and IV melanites as well as in the less Ti-rich schorlomites (Fig. 6a). No correlation between Al and Si exists in garnets of Groups I, II, and IV, though one does exist in Group III (Fig. 6b). However, there is a general trend of slightly increasing Al with decreasing Si from Groups IV to II to I. Group IIA melanites have Al contents that are similar to those of Group I and are generally higher than those of the other melanites. Within the more Ti-rich schorlomites, Fe^{3+} decreases with increasing Si, reflecting Fe^{3+} substitution for Si in the tetrahedral site. In the melanites, there is a strong positive correlation between Fe^{3+} and Si, indicating increasing Fe^{3+} substitution for Ti in the octahedral site of the melanites. Zoning, with F both increasing and decreasing from outer to inner rim, is found in Group III fluoro-hydrograndites. The following trends are found in these garnets: Si decreases and Al increases as F increases, and Al is inversely correlated with Fe^{3+} (Fig. 7). These trends indicate that as the fluoro-hydrogrossular component increases, the andradite component decreases. The Group III garnets show a small variation in Ti content, and no correlation of Ti^{4+} with F was found. Group IV garnets lie on the extensions of the trends defined by Groups I and II (Fig. 6).

Single-crystal X-ray examination was made of three garnet crystals from sample 1-166B. A dark-brown, homogeneous-appearing crystal possesses cubic symmetry with a = 12.144 Å, a value consistent with those of Ti-rich melanites (12.104 to 12.125 Å) and schorlomites (12.138 to 12.167 Å, Deer et al., 1982, p. 626–627). A light-brown crystal gave a = 12.048 Å, suggestive of a Ti-rich andradite (a = 12.029 Å, Deer et al., 1982, p. 624). The third garnet crystal examined is nearly colorless and possesses space group symmetry *Ia3d* with a = 12.067 Å. The very light color and fairly large unit-cell edge suggest that the crystal contains a significant amount of F and OH in the structure. The replacement of SiO_4 groups with $(OH)_4$ and F_4 groups in the garnet crystal structure is expected to expand the lattice; for example, naturally occurring grossulars have a dimensions of 11.790 to 11.94 Å (Deer et al., 1982, p. 604–607), whereas synthetic end-member hydrogrossular, $Ca_3Al_2(OH)_{12}$, has an a dimension of 12.573 Å (Weiss and Grandjean, 1964). The X-ray data are consistent with microprobe analyses that verified that sample 1-166B contains schorlomite, melanite, and fluoro-hydrograndite garnets.

Phlogopites and biotites

Phlogopite and biotite are most commonly observed replacing clinopyroxene and are rarely seen as aggregates

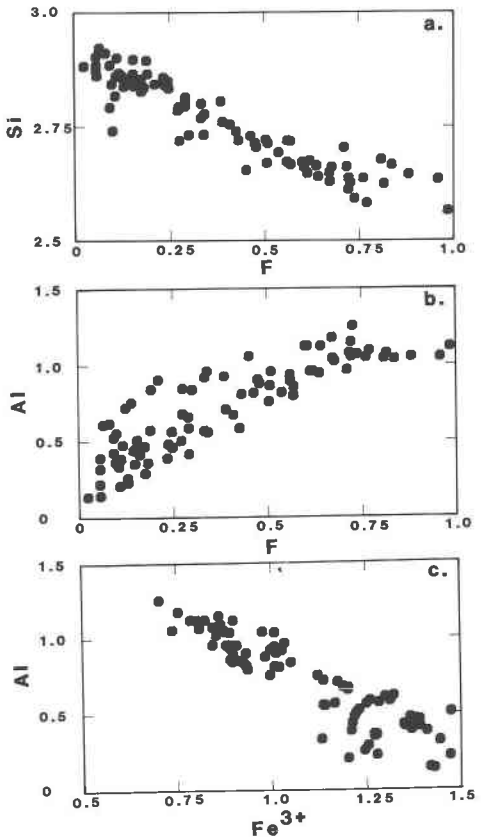

Fig. 7. Variation of (a) Si and (b) Al with F (per formula unit) and (c) variation of Al with Fe^{3+} for Group III fluoro-hydrograndites (cations per 12 anions; see App. 1 for the method of cation calculation) from ijolite xenoliths.

within the groundmass of the ijolite xenoliths. The micas are pleochroic in various shades of green and red or brown. Extinction is often patchy. A large range of mica compositions is found in the ijolite xenoliths from phlogopites with Mg/(Mg + Fe^{2+}) as high as 0.783 to biotites with Mg/(Mg + Fe^{2+}) as low as 0.095. Representative analyses are given in Table 7, and five analyses from 84-1-RSS-B are presented to illustrate the range of compositions in a single sample. Compositions are correlated with color: in general, brown or red-brown grains are more Mg-rich than green grains. However, deep-red biotites (Table 7, no. 6) in 6-DJ7 contain very high Fe and are deficient in (Si + Al) in the tetrahedral site, suggesting that they may contain small amounts of Fe^{3+} in this site, as identified by Dyar and Burns (1986) in other biotites. Ba was detected only in phlogopites from sample 84-1-RSS-B. Most of the micas have <2.5 wt% TiO_2, but some have as much as 4.6 wt% TiO_2. There is no clear correlation of Ti with Mg/(Mg + Fe^{2+}), but very Fe-rich biotites generally contain the most Ti. As expected (see Spear, 1984, and Munoz, 1984, for discussions of the partitioning of F in micas), F is positively correlated with Mg/(Mg + Fe^{2+}) (Fig. 9) in micas from the ijolite xenoliths, but phlogopites from the inner-ring ijolites, with a very nar-

TABLE 5. Garnets from ijolite xenoliths, Diamond Jo quarry

	Group I		Group IIA	Group II		Group IV		
Sample:	3-DJ7-2	1-143B-3	5-DJ7-2A	3-DJ7-2	84-1-RSS-B1	1-143B-3	4-DJ7-2	3-DJ7-2
	1	2	3	4	5	6	7	8
				Weight percent				
SiO_2	25.4	24.7	30.2	32.2	31.0	34.7	34.6	34.8
TiO_2	17.8	17.5	10.3	6.51	9.09	2.64	3.17	1.95
ZrO_2	na	0.80	0.44	0.26	0.22	0.07	0.18	0.14
Al_2O_3	3.26	3.57	3.89	2.24	2.51	1.18	0.79	0.85
V_2O_3	0.59	0.52	0.78	0.54	na	0.39	0.44	1.18
Fe_2O_3*	17.3	17.6	17.8	23.8	22.1	27.1	27.4	27.6
FeO*	2.66	1.87	2.58	1.14	0.90	0.08	0.10	0
MnO	0.46	0.33	0.41	0.70	0.59	0.31	0.29	0.16
MgO	1.28	1.42	1.00	0.64	0.89	0.24	0.24	0.24
CaO	31.4	31.7	31.7	32.1	32.7	33.2	33.5	33.4
Na_2O	0.16	0.10	0.06	0.09	0.09	0.12	0.13	0.09
Nb_2O_5	na	nd	nd	nd	na	nd	nd	nd
F	na	nd	nd	nd	na	nd	nd	0.18
Sum	100.3	100.1	99.16	100.2	100.0	100.0	100.8	100.5†
				Tetrahedral sites				
Si	2.148	2.096	2.547	2.703	2.602	2.912	2.888	2.914
Al	0.325	0.357	0.387	0.222	0.248	0.088	0.078	0.084
Fe^{3+}	0.527	0.547	0.066	0.075	0.150	0	0.034	0.002
	3.000	3.000	3.000	3.000	3.000	3.000	3.000	3.000
				Octahedral sites				
Al	0	0	0	0	0	0.029	0	0
Ti	1.132	1.117	0.653	0.411	0.574	0.167	0.199	0.123
Zr	—	0.038	0.021	0.012	0.010	0.003	0.008	0.007
V	0.040	0.035	0.053	0.036	—	0.026	0.029	0.079
Fe^{3+}	0.574	0.574	1.062	1.429	1.243	1.713	1.689	1.736
Fe^{2+}	0.093	0.056	0.085	0.032	0.062	0.006	0.007	0
Mg	0.161	0.180	0.126	0.080	0.111	0.030	0.030	0.030
Mn	0	0	0	0	0	0.022	0.021	0.011
Ca	0	0	0	0	0	0.004	0.017	0.014
	2.000	2.000	2.000	2.000	2.000	2.000	2.000	2.000
				Dodecahedral sites				
Fe^{2+}	0.095	0.077	0.097	0.048	0.001	0	0	0
Mn	0.033	0.024	0.029	0.050	0.042	0	0	0
Ca	2.845	2.882	2.865	2.887	2.941	2.981	2.979	2.986
Na	0.026	0.016	0.010	0.015	0.015	0.020	0.021	0.015
	2.999	2.999	3.001	3.000	2.999	3.001	3.000	3.001
No. pts. averaged	5	4	4	4	4	3	5	4

Note: nd = not detected. na = not analyzed. Column headings as follows: 1, 2—Euhedral to subhedral schorlomites rimmed by melanites and fluorohydrograndites; 3—Subhedral melanite; 4—Light-red-brown zone surrounding schorlomite no. 1; 5—Light-red melanite in groundmass; 6—Outer zone of colorless overgrowth on schorlomite no. 2; 7—Pale pink skeletal grain in groundmass intergrown with magnetite, aegirine, and calcite; 8—Outer zone of colorless overgrowth on schorlomite no. 1.

* Fe^{3+} and Fe^{2+} calculated by assuming ideal stoichiometry of 8 cations per 12 oxygens.

† Oxide sum adjusted for oxygen equivalent of F.

row range of $Mg/(Mg + Fe^{2+})$, do not show such a correlation. Cl was not detected in any of the micas analyzed.

An unusual intergrowth of biotite, pyrrhotite, ilmenite, minor sphene, and a trace of pyrite occurs in sample 84-1-RSS-A2. The biotite, dark olive green to slightly pleochroic red brown, is Fe-rich and contains 2.48–2.98 wt% V_2O_3 (Table 7, no. 7). Sums for analyses of this biotite were consistently high, probably indicating analytical error, but V-free biotites analyzed during the same analysis session gave good results. Biotites from several of the other xenoliths were analyzed for V, but it was not detected.

Other minerals

Sphene. Sphene occurs as subhedral to euhedral crystals in the groundmass of several ijolite xenoliths, as replacement rims on perovskite (4-DJ7), and as small anhedral grains intergrown with biotite and garnet. Sphene commonly shows pink to colorless pleochroism. Sphene compositions are varied among the ijolite xenoliths (Table 8). The low oxide sums may be attributed to the presence of water and/or unanalyzed elements. Fe is reported as all Fe^{3+} in accordance with the findings of Higgins and Ribbe (1976). We consistently found that Fe^{3+} and Al are inversely correlated with Ti, indicating that these two elements are substituting for Ti in the octahedral site.

Oxides. Primary magnetite occurs with diopside and as inclusions in garnet in 6-DJ7 (Table 9, nos. 1–3), and secondary magnetite is intergrown with aegirine in the groundmass of 4-DJ7. Rims of primary grains are slightly enriched in Ti relative to cores. Laths of Ti-free magnetite (Table 9, no. 4) within clinopyroxene in 4-DJ7 are

Table 6. Fluoro-hydrograndites of Group III from ijolite xenoliths, Diamond Jo quarry

Sample:	1-166B-1	1-143B-3	3-DJ7-2	84-1-RSS-B1	
	1	2	3	4	5
			Weight percent		
SiO_2	31.7	34.7	33.7	31.8	33.6
TiO_2	2.47	2.35	3.36	1.76	3.47
ZrO_2	0.09	0.05	nd	0.12	0.41
Al_2O_3	10.9	9.04	7.72	11.2	4.87
V_2O_3	0.44	0.27	0.28	0.21	0.17
Fe_2O_3*	13.9	17.0	17.7	15.0	21.3
FeO*	0	0	0	0	0
MnO	0.08	0.16	0.13	0.12	0.23
MgO	0.19	0.18	0.26	0.18	0.29
CaO	36.3	35.1	35.3	35.8	34.4
Na_2O	0.04	0.03	0.05	0.07	0.12
Nb_2O_5	nd	nd	nd	nd	nd
F	2.94	1.02	1.10	3.13	1.09
Sum	99.05	99.90	99.60	99.39	99.95
$-F \equiv O$	−1.24	−0.43	−0.46	−1.32	−0.46
Sum	97.81	99.47	99.14	98.07	99.49
(H_2O)†	2.19	0.53	0.86	1.93	0.51
			Tetrahedral sites		
Si	2.471	2.778	2.707	2.481	2.749
OH/4	0.285	0.070	0.115	0.256	0.068
F/4	0.181	0.065	0.070	0.193	0.071
Al	0.063	0.089	0.108	0.070	0.112
	3.000	3.000	3.000	3.000	3.000
			Octahedral sites		
Al	0.939	0.766	0.623	0.961	0.357
Ti	0.145	0.142	0.203	0.103	0.213
Zr	0.003	0.002	—	0.005	0.019
V	0.028	0.017	0.018	0.013	0.011
Fe^{3+}	0.815	1.024	1.070	0.882	1.311
Mn	0.005	0.011	0.009	0.008	0.016
Mg	0.022	0.021	0.031	0.021	0.035
Ca	0.038	0.016	0.046	0.007	0.033
	1.995	1.999	2.000	2.000	1.995
			Dodecahedral sites		
Ca	2.994	2.995	2.992	2.990	2.981
Na	0.006	0.005	0.008	0.011	0.019
	3.000	3.000	3.000	3.001	3.000
Sum	7.995	7.999	8.000	8.000	7.995
F	0.725	0.258	0.279	0.773	0.282
OH	1.139	0.281	0.461	1.024	0.270
O	10.136	11.461	11.260	10.203	11.448
No. pts. averaged	6	4	5	4	3

Note: See App. 1 for detailed explanation of the method used to calculate cations for fluoro-hydrograndites. nd = not detected. Columns are as follows: 1—Outer zone of overgrowth; 2—Inner zone of overgrowth on schorlomite no. 2, Table 5; the outer zone of this overgrowth is colorless melanite (Table 5, no. 6); 3—Inner zone of overgrowth on melanite (Table 5, no. 4); the outer zone of this overgrowth is the V-rich garnet given in Table 5, no. 8; 4, 5—Averages of the outer and inner zones of an overgrowth on a groundmass melanite (Table 5, no. 5).

* All Fe converted to Fe^{3+}.

† H_2O calculated by difference from 100%.

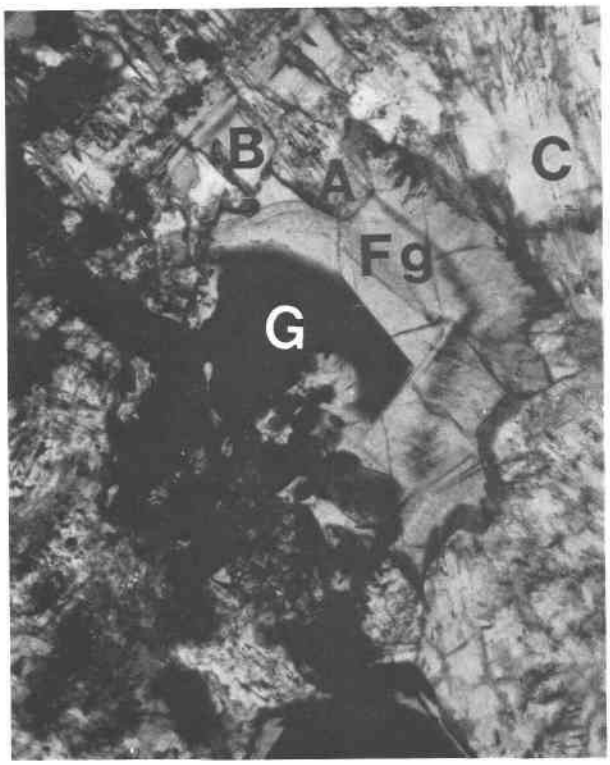

Fig. 8. Zoned fluoro-hydrograndite overgrowth on melanite garnet in ijolite xenolith 1-166B. Field of view is 1.5 mm across the long dimension; plane-polarized light. G = melanite garnet, Fg = fluoro-hydrograndite, B = biotite, A = apatite, C = cancrinite.

partially replaced by pyrrhotite. Laths of pyrrhotite occur within garnet and clinopyroxene in other samples, indicating that replacement of magnetite by the sulfide was complete.

Polysynthetically twinned perovskite is purple-brown and occurs as rounded inclusions in clinopyroxene (4-DJ7), as blebs being replaced by garnet (6-DJ7), and as grains rimmed by sphene within the altered groundmass of 4-DJ7. Perovskites in both samples have essentially identical compositions (Table 9, nos. 5, 6) and low amounts of all minor elements. Ilmenite intergrown with pyrrhotite and biotite in 84-1-RSS-A2 is Mn-rich (Table 9, no. 7) and contains minor amounts of V.

Apatite. Compositions (Table 10) and textural relationships indicate that two generations of apatites are present. Apatites of both groups are inclusion-rich. Representative grains from both groups were analyzed in three samples. The early-formed apatites occur as euhedral, equant inclusions in clinopyroxene and schorlomite garnet and contain less F than late-formed acicular (up to 7 mm long) to tabular grains observed in the groundmass. Zoning was not detected in either group.

Cancrinite, natrolite, and nepheline. Cancrinite and natrolite, in addition to calcite, replace most of the nepheline and form most of the groundmass of the ijolite xenoliths. Analyses are given in Table 11. Natrolite and cancrinite were also confirmed optically and by using X-ray powder diffraction. Nepheline that is only partially replaced by cancrinite, however, occurs in 5-DJ7 and 6-DJ7. Nepheline compositions lie within the Morozewicz-Buerger convergence field (Tilley, 1954); the analysis in Table

TABLE 7. Biotites and phlogopites from ijolite xenoliths, Diamond Jo quarry

Sample:	84-1-RSS-B					6-DJ7-1	84-1-RSS-A2
	1	2	3	4	5	6	7
			Weight percent				
SiO_2	37.3	36.6	35.1	33.4	32.7	33.4	34.4
TiO_2	1.93	0.98	1.80	1.42	3.74	1.98	1.52
Al_2O_3	15.4	15.3	13.7	14.7	14.0	12.0	13.8
V_2O_3	na	na	na	na	na	na	2.70
FeO	11.6	17.2	24.9	32.1	34.1	35.3	28.8
MnO	0.23	0.40	0.52	0.74	0.63	1.55	0.66
MgO	18.6	14.9	9.72	4.99	2.35	2.18	6.08
CaO	0.07	nd	0.11	nd	0.06	nd	nd
BaO	0.54	nd	nd	nd	nd	nd	nd
Na_2O	0.20	0.09	0.14	0.06	0.12	0.09	0.11
K_2O	10.0	10.1	9.72	9.51	9.41	9.20	9.54
F	1.45	0.82	0.53	0.13	nd	nd	nd
Sum	97.32	96.39	96.24	97.05	97.11	95.70	97.61
$-F \equiv O$	−0.61	−0.35	−0.22	−0.05			
Sum	96.71	96.04	96.02	97.00			
			Cations				
Si	2.750	2.773	2.770	2.701	2.675	2.802	2.730
Al	1.250	1.227	1.230	1.299	1.325	1.190	1.270
	4.000	4.000	4.000	4.000	4.000	3.992	4.000
Al	0.085	0.139	0.045	0.102	0.022	0	0.021
Ti	0.107	0.056	0.107	0.086	0.230	0.125	0.091
V	—	—	—	—	—	—	0.171
Fe	0.717	1.089	1.643	2.173	2.334	2.477	1.911
Mn	0.014	0.026	0.035	0.051	0.044	0.110	0.044
Mg	2.046	1.682	1.145	0.602	0.286	0.272	0.718
	2.929	2.992	2.975	3.014	2.916	2.984	2.956
Ca	0.006	0	0.009	0	0.005	0	0
Ba	0.016	0	0	0	0	0	0
K	0.942	0.979	0.980	0.981	0.981	0.984	0.964
Na	0.029	0.013	0.020	0.009	0.019	0.015	0.017
	0.993	0.992	1.009	0.990	1.005	0.999	0.981
Sum	7.962	7.984	7.984	8.004	7.921	7.975	7.937
F*	0.338	0.196	0.132	0.033	—	—	—
Molar $Mg/(Mg + Fe^{2+})$	0.740	0.607	0.411	0.217	0.109	0.099	0.273

Note: Cations calculated to 11 oxygen equivalents assuming all Fe as Fe^{2+}. nd = not detected. na = not analyzed. Columns are as follows: 1 to 5—Single-point analyses of phlogopite and biotite replacing pyroxene; 6—Bright-red biotite intergrown with magnetite replacing pyroxene (3-point average); 7—Biotite intergrown with ilmenite and pyrrhotite (6-point average).

* F per formula unit calculated by assuming (OH + F) = 2.

11 has a composition of $Ne_{74.1}Ks_{25.4}Qtz_{0.50}$, indicating crystallization or equilibration at temperatures <500 °C (Hamilton, 1961). Such low temperatures suggest postcrystallization re-equilibration. Calcite was analyzed qualitatively using energy-dispersive analysis on the microprobe, and Sr was the only minor element detected.

Single-crystal X-ray examination of cancrinite from sample 1-166B gave the following crystallographic data: hexagonal, space group $P6_3$, a = 12.63 Å, and c = 5.118 Å, indicating that the crystal is composed for the most part of layers in AB AB stacking. However, weak reflections appear at nonintegral values along reciprocal-lattice row lines parallel to c^*, indicating that the cancrinite structure has some sort of stacking disorder; for example, see Rinaldi and Wenk (1979).

PETROGRAPHY AND MINERAL COMPOSITIONS OF THE INNER-RING IJOLITES

Preliminary study of the inner-ring ijolites is summarized here. Sample 99423/6 is from the east side of the main body of biotite-garnet ijolite, and sample 99423/7 is from the main body of garnet ijolite located approximately 1.1 km north of Diamond Jo quarry (Fig. 1). The modes of these samples, which were collected by F. C. Calkins of the U.S. Geological Survey in 1918, are given in Table 3. Samples of inner-ring ijolite collected as part of this study include garnet ijolite 85-13B-RSS and biotite-garnet ijolite 85-16-RSS (Fig. 1). Neither of the biotite-garnet ijolites studied contains any clinopyroxene; however, Erickson and Blade (1963) did report a very minor amount of diopside in one of their samples. Clinopyroxene may have been totally altered to biotite in most of the rock.

Garnet ijolite

Garnet ijolite (sample 99423/7, Fig. 4c) is texturally more similar to the finest-grained ijolite xenolith from Diamond Jo (sample 6-DJ7) than to the coarser-grained xenoliths. The silicates and oxides in 99423/7 form aggregates in places, with the silicates normally surrounding

TABLE 8. Sphenes from ijolite xenoliths, Diamond Jo quarry

Sample:	4-DJ7-2	3-DJ7-2	1-166B-1
	1	2	3
	Weight percent		
SiO_2	29.4	30.3	30.2
TiO_2	34.2	38.4	35.5
ZrO_2	0.21	0.10	0.83
Al_2O_3	1.35	0.21	1.18
V_2O_3	0.71	0.38	0.29
Fe_2O_3*	2.74	0.94	1.90
MnO	nd	nd	nd
MgO	0.16	0.16	0.15
CaO	27.9	28.4	28.4
Na_2O	0.04	0.15	0.07
Nb_2O_5	0.56	nd	nd
F	1.07	0.45	0.66
Sum	98.34	99.49	99.18
$-F \equiv O$	−0.45	−0.19	−0.28
Sum	97.89	99.30	98.90

Note: nd = not detected. Each analysis reported is a 3-point average. Columns are as follows: 1—Overgrowth on perovskite; 2—Euhedral grain in the groundmass; 3—Subhedral grain in the groundmass within an "atoll" garnet.

* All Fe reported as Fe^{3+}.

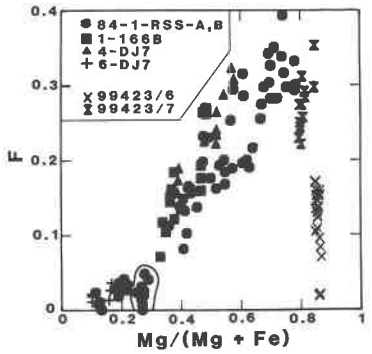

Fig. 9. Variation of F (per formula unit of 11 anions) with Mg/(Mg + Fe) in phlogopites and biotites from ijolite xenoliths, garnet ijolite 99423/7, and biotite-garnet ijolite 99423/6. Circled analyses from sample 84-1-RSS-A are of V-bearing biotites intergrown with ilmenite and pyrrhotite.

the oxides. The garnet ijolite contains laths of diopside, some of which are twinned, interstitial to, and included within anhedral to equant grains of nepheline. The diopsides (Table 12) contain less Al and Ti than do the diopsides from the ijolite xenoliths, but the same correlations between Al, Ti, and Mg/(Mg + Fe^{2+} + Fe^{3+}) are observed (Figs. 5a, 5b). Garnet is continuously zoned, from red-brown cores of melanite composition with moderate Ti contents to golden-brown rims with a lower Ti content (Table 12, nos. 3, 4). Phlogopites are pleochroic (light to dark brown) and some grains have green rims that are depleted in Ti relative to the brown cores (Table 12, nos. 12, 13). Cores and rims have essentially the same Mg/(Mg + Fe^{2+}) ratio, with an overall range of 0.798 to 0.850, and there is no correlation of that ratio with F as was found in micas from the ijolite xenoliths (Fig. 9). However, F does show a strong positive correlation with Ti in the phlogopites from the garnet ijolite; such a correlation was not found in micas from the ijolite xenoliths. Nepheline is essentially unaltered, unlike nepheline in the ijolite xenoliths. Perovskite is common and is intergrown with and rimmed by both magnetite and garnet. Magnetite in the garnet ijolite is homogeneous (Table 13, no. 1). The overall Nb content of the perovskites (Table 13, nos. 4, 5) ranges from 0.63 to 1.82 wt% Nb_2O_5, and Nb

TABLE 9. Oxides from ijolite xenoliths, Diamond Jo quarry

Sample:	Magnetite				Perovskite		Ilmenite
	6-DJ7-1			4-DJ7-2	6-DJ7-1	4-DJ7-2	84-1-RSS-A2
	1	2	3	4	5	6	7
				Weight percent			
SiO_2	nd	nd	nd	nd	nd	nd	nd
TiO_2	8.80	7.97	11.6	0.04	54.8	55.2	50.6
Al_2O_3	0.78	0.82	0.32	nd	0.16	0.14	0.05
La_2O_3	na	na	na	na	0.57	0.46	na
V_2O_3	0.77	0.77	0.80	0.03	0.54	0.60	0.59
Fe_2O_3*	50.1	51.5	44.2	68.0	—	—	2.48
FeO*	36.8	36.7	39.2	30.7	1.21	0.87	37.4
MnO	2.19	1.69	2.14	nd	0.22	0.17	7.97
MgO	0.11	0.07	0.03	nd	0.23	0.24	0.06
CaO	0.05	nd	nd	nd	40.3	40.5	nd
SrO	na	na	na	na	0.28	0.21	na
Na_2O	na	na	na	na	0.35	0.17	na
Nb_2O_5	nd	nd	nd	nd	0.72	0.78	nd
Sum	99.60	99.52	98.30	98.77	99.38	99.34	99.15
No. pts. averaged	3	3	3	3	6	6	6

Note: nd = not detected; na = not analyzed. Cr analyzed for but not detected in magnetite and ilmenite; Zr analyzed for but not detected in perovskite. Columns are as follows: 1, 2—Rim and core, respectively, of groundmass grain; 3—Inclusion in garnet; 4—Magnetite with pyrrhotite lath within clinopyroxene; 5—Perovskite being replaced by garnet; 6—Perovskite being replaced by sphene; 7—Ilmenite intergrown with V-bearing biotite and pyrrhotite.

* Fe^{3+} and Fe^{2+} calculated by assuming ideal stoichiometry of 3 cations per 4 oxygens for magnetites and 2 cations per 3 oxygens for ilmenite; all Fe as Fe^{2+} for perovskite.

TABLE 10. Apatites from ijolite xenolith, Diamond Jo quarry

Sample:	84-1-RSS-B1	
	1	2
	Weight percent	
SiO_2	0.18	0.69
La_2O_3	nd	0.08
Ce_2O_3	0.11	0.14
FeO	0.13	0.17
MnO	nd	nd
MgO	0.13	0.13
CaO	55.0	55.3
SrO	0.65	0.56
BaO	nd	nd
Na_2O	0.03	0.03
P_2O_5	41.1	39.4
F	3.71	2.75
Cl	nd	nd
Sum	101.04	99.25
$-F \equiv O$	−1.56	−1.16
Sum	99.48	98.09

Note: nd = not detected. Columns are as follows: 1—3-point average of a grain from the groundmass. 2—3-point average of inclusions within clinopyroxene.

TABLE 11. Nepheline and alteration products from ijolite xenoliths, Diamond Jo quarry

	Cancrinite	Natrolite	Nepheline
Sample:	1-166B-1	1-166B-1	5-DJ7-2A
	Weight percent		
SiO_2	34.4	46.0	40.8
Al_2O_3	28.8	27.1	35.4
FeO	0.07	0.08	0.70
MnO	nd	nd	nd
MgO	0.08	0.05	nd
CaO	7.67	0.23	0.11
Na_2O	17.1	14.9	15.9
K_2O	0.04	0.26	7.28
Sum	88.16	88.62	100.20

Note: nd = not detected.

is enriched in cores relative to rims. Minor amounts of pyrrhotite are found, commonly included within perovskite.

Garnet ijolite 85-13B-RSS has a variable texture (Fig. 4d) in which laths of diopside form aggregates. Other parts of the same sample are texturally more similar to sample 99423/7 (Fig. 4c) and have similar proportions of pyroxene and nepheline. Preliminary microprobe data from garnet ijolite 85-13B-RSS show that this sample is slightly more evolved than ijolite 99423/7. The same zoning trends are found in diopsides from 85-13B-RSS, but overall the diopsides are more Fe-rich with a range of $Mg/(Mg + Fe^{2+} + Fe^{3+})$ from 0.660 to 0.753. Garnets, which are more abundant than in 99423/7, are zoned from cores of schorlomite composition to rims of melanite composition. Nepheline is essentially unaltered. Perovskite and magnetite are not found, and pyrrhotite is more abundant than in 99423/7. Biotite, pyrite, calcite, and apatite are observed as minor phases.

Biotite-garnet ijolite

Both samples of biotite-garnet ijolite (sample 99423/6 was originally termed "biotite ijolite" by Calkins but was collected from an area mapped as biotite-garnet ijolite by Erickson and Blade, 1963) are coarse grained and texturally distinct from the ijolite xenoliths and the inner-ring garnet ijolites. Pyroxene was not found in either sample studied. Garnet from sample 99423/6 is intergrown with and rims magnetite and also replaces perovskite. It has a wider range of compositions (Table 12, nos. 5–8) than garnets from the garnet ijolite but exhibits similar optical and chemical zoning (dark-red, Ti-rich cores to golden-brown, less Ti-rich rims). Anhedral yellow to nearly colorless garnet is intergrown with calcite and phlogopite. Phlogopites from 99423/6 have pleochroic brown cores and green rims, are optically and chemically similar (Table 12, nos. 9, 10) to phlogopites from garnet ijolite 99423/7, and have an overall range of $Mg/(Mg + Fe^{2+})$ from 0.850 to 0.867. Brown phlogopite in the biotite-garnet ijolite is, on the average, slightly less Ba-rich and Fe-rich than that in the garnet ijolite. Phlogopites from both of the inner-ring ijolites are distinct from micas from the ijolite xenoliths (Fig. 9). Nepheline is partially altered to a material that forms very fine grained, brown, felted masses and that contains laths of light-green phlogopite (Table 12, no. 11). This phlogopite is more aluminous and contains more Ba, but less F and Ti, than the green phlogopite that rims groundmass phlogopite, indicating that the two green micas are not contemporaneous. Magnetite rims both perovskite and phlogopite and has a wider range of compositions than magnetite from the garnet ijolite. It is depleted in Ti where it is in contact with perovskite (Table 13, nos. 2, 3). Perovskite from 99423/6 has a smaller range of Nb_2O_5 contents (0.34–1.13 wt%; Table 13, no. 6) than was found in perovskite from the garnet ijolite.

Biotite-garnet ijolite 85-16-RSS is texturally like sample 99423/6, and preliminary microprobe data indicate that mineral compositions in these two samples are essentially the same. Zeolite, belonging to the thomsonite-gonnardite series, partially replaces nepheline.

DISCUSSION

Relationships between the ijolite xenoliths and inner-ring ijolites

Erickson and Blade (1963), on the basis of field relationships, concluded that at least some of the inner-ring ijolites from Magnet Cove were younger than the garnet-pseudoleucite syenite and other alkaline syenites that form the outer ring of the complex. The ijolite xenoliths—which occur within garnet-pseudoleucite syenite at Diamond Jo quarry and hence must be older than this syenite—were not considered by Erickson and Blade (1963) in their discussion of age relationships because these xenoliths appeared to be megascopically distinct from the inner-ring ijolites. Ijolites from other alkaline igneous complexes are also mineralogically and chemically heterogeneous. In some complexes, such as Usaki and Homa Mountain,

TABLE 12. Silicates from garnet ijolite 99423/7 and biotite-garnet ijolite 99423/6, Magnet Cove igneous complex, Arkansas

	Pyroxene		Garnet*						Phlogopite				
			II	IV	II	II	II	IV					
Sample:	99423/7		99423/7		99423/6				99423/6			99423/7	
	1	2	3	4	5	6	7	8	9	10	11	12	13
							Weight percent						
SiO_2	52.8	48.5	33.1	34.7	27.0	30.3	34.1	35.6	37.7	38.3	37.8	36.1	38.3
TiO_2	0.18	1.60	6.24	2.68	14.8	11.3	3.63	0.94	1.46	0.50	0.38	2.23	0.83
ZrO_2	na	na	nd	nd	0.76	nd	nd	nd	na	na	na	na	na
Al_2O_3	0.71	3.94	2.26	1.93	1.64	1.81	2.35	2.80	15.4	15.6	17.9	15.2	15.4
V_2O_3	nd	nd	0.34	0.28	0.42	0.22	0.29	0.19	nd	nd	nd	0.08	0.06
Fe_2O_3**	2.97	5.97	23.1	26.7	19.5	20.0	25.0	26.1	—	—	—	—	—
FeO**	2.67	2.90	1.13	0.02	1.76	1.48	0.33	0.01	6.98	6.91	6.42	9.24	7.33
MnO	0.40	0.36	0.30	0.26	0.36	0.39	0.34	0.30	0.39	0.37	0.42	0.38	0.40
MgO	15.0	12.6	0.92	0.63	1.48	1.45	0.72	0.46	22.9	23.6	23.1	21.0	23.1
CaO	24.8	23.7	32.8	33.2	32.0	32.6	32.8	33.0	nd	nd	nd	nd	nd
BaO	na	na	na	na	na	na	na	na	0.70	0.62	1.07	1.22	0.98
Na_2O	0.36	0.69	0.05	nd	0.07	0.06	nd	nd	0.26	0.25	0.16	0.09	0.07
K_2O	nd	nd	na	na	na	na	na	na	9.70	9.88	9.43	9.53	9.39
Nb_2O_5	na	na	nd	nd	nd	0.06	nd	nd	na	na	na	na	na
F	na	na	nd	nd	nd	nd	nd	nd	0.66	0.63	nd	1.02	1.43
Sum	99.89	100.3	100.2	100.4	99.79	99.67	99.56	99.40	96.15	96.66	96.68	96.09	97.29
$-F\equiv O$									−0.28	−0.26		−0.43	−0.60
Sum									95.87	96.40		95.66	96.69
No. pts. averaged	3	3	5	3	3	4	4	3	3	3	3	3	3

Note: nd = not detected. na = not analyzed. Columns are as follows: 1, 2—Core and rim, respectively, of pyroxene lath; 3, 4—Red core and lighter-colored rim, respectively, of garnet; 5 through 8—Darker-red core, lighter-red zone, yellow zone, and colorless rim, respectively, of garnet; 9, 10—Brown core and green rim, respectively, of phlogopite; 11—Green laths of phlogopite in altered nepheline; 12, 13—Brown core and green rim, respectively, of phlogopite.

* Roman numerals refer to garnet group designations as defined in the text.

** Fe^{3+} and Fe^{2+} calculated by assuming 4 cations per 6 oxygens for pyroxenes and by assuming 8 cations per 12 oxygens for garnets; all Fe as Fe^{2+} for phlogopites.

Kenya (Le Bas, 1977), more than one intrusion of ijolite occurred. Progressive crystallization with late-stage deuteric or metasomatic alteration also accounts for some of the observed heterogeneities in ijolites from these complexes. Mitchell and Brunfelt (1975) concluded that rocks of the urtite-ijolite-melteigite series at the Fen complex, Norway, are related by low-pressure differentiation of a single parent magma.

The ijolite xenoliths and garnet ijolite from the inner ring of Magnet Cove have similar mineral and chemical characteristics. The trace-element composition of the biotite-garnet ijolite, in particular its REE pattern and its high concentrations of Nb, Ba, and Sr, set it apart from all the other Magnet Cove ijolites. Additional data are required to fully assess the petrogenetic relationship between the ijolite xenoliths and inner-ring ijolite and to determine if more than one ijolite magma was present.

Clinopyroxenes from garnet ijolite 99423/7 (and also 85-13B-RSS), although more magnesian than those from the ijolite xenoliths, lie along the same trend defined by xenolith pyroxenes on the plot of Al vs. $Mg/(Mg + Fe^{2+} + Fe^{3+})$ (Fig. 5b). Two trends are found on the Al-Ti plot of clinopyroxene compositions (Fig. 5a); one is formed by the ijolite xenoliths excluding 6-DJ7, and the second is formed by 6-DJ7 and inner-ring ijolite 99423/7. Some analyses, particularly from xenoliths 4-DJ7 and 1-143A, are intermediate between the two trends, suggesting that

TABLE 13. Oxides from garnet ijolite 99423/7 and biotite-garnet ijolite 99423/6, Magnet Cove igenous complex, Arkansas

	Magnetite			Perovskite		
Sample:	99423/7	99423/6		99423/7		99423/6
	1	2	3	4	5	6
			Weight percent			
TiO_2	4.26	2.76	6.29	56.4	55.5	57.1
ZrO_2	na	na	na	0.06	nd	na
Al_2O_3	0.83	0.89	1.46	0.07	0.04	0.05
V_2O_3	0.77	0.68	0.70	0.60	0.55	0.57
La_2O_3	na	na	na	0.25	0.49	na
Fe_2O_3*	59.6	62.4	55.1	—	—	—
FeO*	30.6	27.3	28.0	0.78	0.96	0.93
MnO	2.15	2.83	4.81	0.14	0.08	nd
MgO	1.45	2.13	2.66	0.23	0.22	0.22
CaO	nd	0.05	nd	40.6	40.1	40.3
SrO	na	na	na	0.31	0.39	na
Na_2O	na	na	na	0.23	0.39	na
Nb_2O_5	nd	nd	0.06	0.75	1.57	0.85
	99.66	99.04	99.08	100.4	100.3	100.0
No. pts. averaged	8	3	3	6	4	3

Note: nd = not detected. na = not analyzed. Cr analyzed for but not detected in both magnetites and perovskites. Columns are as follows: 1—Magnetite replacing and intergrown with perovskite, range of TiO_2 is 3.73 to 5.28 wt%; 2, 3—Rim and core, respectively, of magnetite adjacent to perovskite; 4, 5—Rim and core, respectively, of grain enclosed by magnetite; 6—Perovskite being replaced by magnetite.

* Fe^{3+} and Fe^{2+} calculated by assuming ideal stoichiometry of 3 cations per 4 oxygens for magnetites; all Fe as Fe^{2+} for perovskites.

a continuum in compositions exists. The more Mg-rich diopside compositions found in inner-ring ijolite 99423/7 indicate that it is a less-evolved rock than are the ijolite xenoliths.

Garnets from the inner-ring ijolites belong to Groups I, II, and IV and, if plotted with the garnets from the ijolite xenoliths, would lie along the same trends as these garnets (Fig. 6). Inner-ring ijolite 99423/7 contains garnets that are zoned to less Ti-rich compositions than most of the ijolite xenoliths and also contains significantly more perovskite than do the xenoliths. Perovskite in xenolith 6-DJ7 is almost completely replaced by garnet that is zoned to more Ti-rich compositions than garnet in inner-ring ijolite 99423/7, indicating that with progressive crystallization of the ijolites, early-formed perovskite was replaced by increasingly more Ti-rich garnet.

Magnetites from 6-DJ7 and 99423/7 have similar concentrations of Al, Mn, and V, but 99423/7 magnetites contain more Mg and less Ti, consistent with their coexisting with more magnesian and less titaniferous pyroxenes. Perovskite from the ijolite xenoliths and inner-ring garnet ijolite have similar minor-element concentrations. Perovskites from inner-ring biotite-garnet ijolite 99423/6 appear unaltered and have compositions similar to perovskites from both the ijolite xenoliths and garnet ijolite 99423/7.

Metasomatic minerals

The occurrences of cancrinite, natrolite, calcite, biotite, sodic pyroxenes, and andradite are not unusual as late-stage metasomatic phases in ijolites and associated alkaline rocks. Le Bas (1977) provided detailed petrographic descriptions of a variety of ijolites from the alkaline igneous complexes of the Homa Bay area of Kenya, including those of secondary minerals formed as the result of reaction between magmatic phases and metasomatic fluids derived from intrusion of carbonatite or other alkaline siliceous rocks. In ijolite from the Usaki complex, Le Bas (1977) observed late-stage development of calcite and K-feldspar and replacement of nepheline by cancrinite and natrolite, melanite by andradite, and aegirine-augite by aegirine and biotite. With the exception of the development of K-feldspar, the formation of these metasomatic minerals—which Le Bas attributed to reaction of residual fluids derived from the later intrusion of a wollastonite urtite—parallels that observed in the ijolite xenoliths from Diamond Jo quarry. Secondary minerals, including those just described, are also identified (e.g., by Le Bas, 1977) as forming as the result of deuteric alteration.

The replacement of nepheline by cancrinite and natrolite and of diopside by biotite appear to be contemporaneous reactions. As nepheline reacts with fluids rich in CO_2 and H_2O, K is released that is then free to form biotite. The replacement of diopside releases Ca and minor Si that are then available for the formation of calcite, cancrinite, natrolite, and fluoro-hydrograndite.

Minor amounts of sphene occur in all of the garnet ijolites, but it is not found in the inner-ring ijolites. Sphene forms subhedral to euhedral grains in the groundmass of 4-DJ7 and 6-DJ7, indicating that it crystallized at the same time as the other metasomatic phases. In 4-DJ7, a sample poor in garnet, sphene replaces perovskite. Sphene is also intergrown with biotite and fluoro-hydrogranite in other ijolites, indicating that it formed after primary clinopyroxene ceased crystallizing.

Garnets of the schorlomite-melanite-andradite series are described as being both primary and metasomatic in origin (e.g., Le Bas, 1977; Sørensen, 1974). In the ijolites from Magnet Cove, garnets, with progressively increasing Fe^{3+} and decreasing Ti, span the range from magmatic to metasomatic. In the ijoite xenoliths, garnets of Group I and IIA began crystallizing after nepheline and diopside began to form, and then cocrystallized with diopside. Melanites of Group II may represent an intermediate stage between magmatic and metasomatic crystallization, as they occur both as rims on schorlomites and as grains intergrown with the hydrous alteration products of nepheline. Garnets of Groups III and IV are exclusively associated with other metasomatic minerals and crystallized with them. Garnets of Group III are not found in the ijolites from the inner ring. Low-Ti melanites of Group IV are associated with calcite and biotite in the garnet-biotite ijolites and thus formed with these metasomatic minerals.

The fluoro-hydrograndite formed by the reaction of early-formed garnet with F-rich metasomatic fluids. Occurrences of F in garnet have been reported from several different geologic environments. Nash and Wilkinson (1970) described a melanite garnet containing 0.8 wt% F from a Na-rich syenite in the Shonkin Sag laccolith. Other occurrences of F-bearing garnets are reported from skarns and various types of mineral deposits (Valley et al., 1983; Van Marcke de Lummen, 1986; Dobson, 1982; Yun and Einaudi, 1982; Madel et al., 1987; Gunow et al., 1980). The highest concentration of F in garnet was reported by Madel et al. (1987) who described a spessartine garnet containing up to 3.7 wt% F.

Valley et al. (1983) described grossular garnets with up to 0.76 wt% F from Adirondack calc-silicates. They proposed two substitutions by which F and OH could enter the garnet structure: $[(F,OH)_4]^{4-}$ for $(SiO_4)^{4-}$ and $(Al^{3+}\cdot O^{2-})$ for $[(Mg,Fe)^{2+}(F,OH)^-]$. Our analyses show an inverse correlation of F and Si (Fig. 7), consistent with F_4^{4-} for $(SiO_4)^{4-}$ substitution mechanism. Ca + Na, and in many instances Ca alone, exceeds 3 cations per formula unit, with a concomitant and nearly equal deficiency of octahedrally coordinated cations (Table 6). Crystal-structure determinations of a synthetic deuterated grossular garnet by Forman (1968) verified that $(DO)_4^{4-}$ can completely substitute for $(SiO_4)^{4-}$ and also showed that all three polyhedra, $(DO)_4$, CaO_8, and AlO_6, are larger than the equivalent polyhedra in grossular garnet, $Ca_3Al_2Si_3O_{12}$. It is possible that the introduction of F and OH expands the structure and allows Ca to enter the octahedral site. Although the substitutional mechanism

$(Al^{3+}\cdot O^{2-})$ for $[(Mg,Fe)^{2+}\cdot(OH,F)^{-}]$ proposed by Valley et al. (1983) is crystal-chemically feasible, the low amount of Mg, the lack of correlation of Mg content with F, and the good assumption that no Fe^{2+} is present in the structure lead us to believe that this type of replacement is not important in the Diamond Jo fluoro-hydrograndites.

The unusual intergrowth of pyrrhotite, ilmenite, and V-bearing biotite texturally appears to be a replacement assemblage, not a xenolith. The biotites, except for their V content, fall within the range of compositions of biotites that replace primary clinopyroxene and are Fe-rich (Fig. 9, Table 7), indicating relatively late crystallization. The primary minerals were probably magnetite and clinopyroxene, given that magnetite is partly replaced by pyrrhotite and clinopyroxene is partly replaced by biotite.

The enrichment of V in minerals formed during late-stage metasomatism of the ijolite xenoliths (Group IV garnets, aegirine, biotite) indicates that V either was introduced with externally derived metasomatic fluids or was mobilized during metasomatism. We have found (unpub. data) similar enrichments of V, and also Ti, in late-stage minerals in syenites from Magnet Cove and are currently assessing the significance of such enrichments in relation to the economically important V and Ti deposits of the complex.

Possible sources of the metasomatic fluids

Alkaline igneous rocks and carbonatites are, by their very nature, volatile-rich (Kogarko, 1974). Metasomatic alteration produced by the volatiles associated with the intrusion of these rocks has been well-documented (e.g., Sørensen, 1974; Le Bas, 1977, 1981), and is ascribed to three processes: alkali metasomatism associated with intrusion of carbonatite, metasomatism resulting from intrusion of an alkaline silicate magma, and autometasomatism, or deuteric alteration, in which early magmatic phases react with their own residual fluids to form a suite of secondary, lower-temperature minerals. As different rock units within an alkaline igneous complex may have been emplaced at different times, these three metasomatic processes may be superimposed on one another (Le Bas, 1977).

Metasomatic alteration of the ijolite xenoliths from Diamond Jo quarry may be the result of one or more such processes. Ijolites from other alkaline complexes are volatile-rich and produce metasomatism of adjacent rock during intrusion, as described by Le Bas (1977). At this time, we cannot identify the specific source(s) of the metasomatic fluid(s) responsible for the alteration of the ijolite xenoliths. The metasomatism may, at least in part, be due to reaction with residual ijolitic fluids. The ijolite xenoliths from Diamond Jo quarry occur within garnet-pseudoleucite syenite that is in contact with nepheline syenite (Fig. 2). We (Flohr and Ross, 1987, and unpub. data) have found that the nepheline syenites and garnet-pseudoleucite syenites from Diamond Jo are volatile-rich, with high amounts of F, Cl, CO_2, and H_2O. Metasomatism of the xenoliths may have occurred when they were entrained in the volatile-rich garnet-pseudoleucite magma. The lack of a chilled margin at the contact of the nepheline syenite and the garnet-pseudoleucite syenite indicates that they were emplaced in relatively rapid succession, possibly permitting volatile exchange between the two syenites and causing additional metasomatism of the entrained ijolite xenoliths by fluids from the nepheline syenite.

The alteration observed in the inner-ring biotite-garnet ijolite is different in several respects from that found in the ijolite xenoliths. In the biotite-garnet ijolite, nepheline is altered to thomsonite-gonnardite and minor cancrinite, rather than cancrinite and natrolite; F-free garnet, rather than fluoro-hydrograndite, replaces melanite; sphene is absent, and fluorapatite is rare. Both the ijolite xenoliths and the inner-ring biotite-garnet ijolite contain minor amounts of calcite and abundant biotite. Erickson and Blade (1963) attributed alteration of biotite-garnet ijolite to reaction with carbonatite. Biotite-garnet ijolites are more closely associated with the carbonatite (Fig. 1) than any of the other ijolites studied, making them the most likely to have been altered by the intrusion of the carbonatite. Nelson et al. (1988) reported high concentrations of Ba and Sr in carbonatite from Magnet Cove; infiltration of the biotite-garnet ijolite by carbonatitic fluids may have introduced high concentrations of Ba and Sr into the biotite-garnet ijolite. Inner-ring garnet ijolite is not in contact with any known outcrops of carbonatite, and none of the samples examined in this study are extensively altered. Erickson and Blade (1963) reported that some of the samples of garnet ijolite examined by them contain secondary cancrinite, thomsonite, and calcite. The variable degree of alteration of garnet ijolite indicates that alteration by carbonatitic fluids was not pervasive throughout the Magnet Cove complex. It is therefore unlikely that the metasomatism observed in the ijolite xenoliths and also in the syenites from Diamond Jo quarry (Flohr and Ross, unpub. data) is the result of carbonatitic metasomatism.

The inner-ring ijolites lack abundant F-rich minerals. The parent magma(s) of these ijolites may have been poor in F relative to the magma(s) from which the ijolite xenoliths crystallized. Alternatively, F may have been present, but the volatile-rich portion of the magma(s) separated from the crystallizing ijolites and did not react extensively with them. The F found in minerals in the late-stage metasomatic groundmass of the ijolite xenoliths may have been introduced by syenitic fluids.

Acknowledgments

Henry deLinde (Mabelvale, Arkansas), owner of the Diamond Jo quarry, kindly granted access to it. Mike Howard (Arkansas Geological Commission) and Don Owens (University of Arkansas, Little Rock) helped to collect samples. Mike Howard also provided us with invaluable guidance in locating sampling sites within the Magnet Cove complex. Ted Armbrustmacher (USGS, Denver) provided the portable core drill and helped to collect samples. The National Museum, Washington, D.C., provided

polished thin sections of a suite of samples from the F. C. Calkins collection. Daphne R. Ross (Smithsonian Institution, Department of Mineral Sciences) furnished X-ray powder-diffraction data. M. Kavulak, J. Marinenko, N. Rait, J. Mee, J. Evans, M. Doughton, E. Brandt, J. H. Christie, J. Sharkey, and L. Jackson (USGS) provided whole-rock analyses. Jim McGee (USGS, Reston) gave advice on selection of microprobe standards and guidance in the use of the instrument. Jim McGee, Ted Armbrustmacher, and two anonymous reviewers gave very thoughtful and thorough reviews of this manuscript. This work was funded by the Strategic and Critical Minerals Program of the USGS.

References cited

Albee, A.L., and Ray, L. (1970) Correction factors for election probe micro-analysis of silicates, oxides, phosphates, and sulfates. Analytical Chemistry, 42, 1408–1414.

Baedecker, P.A. (1987) Methods for geochemical analysis. U.S. Geological Survey Bulletin 1770, 127 p.

Bence, A.E., and Albee, A.L. (1968) Empirical correction factors for electron microanalysis of silicates and oxides. Journal of Geology, 76, 382–403.

Cullers, R.L., and Medaris G., Jr. (1977) Rare earth elements in carbonatite and cogenetic alkaline rocks: Examples from Seabrook Lake and Callander Bay, Ontario. Contributions to Mineralogy and Petrology, 65, 143–153.

Deer, W.A., Howie, R.A., and Zussman, J. (1982) Rock-forming minerals, vol. 1A, Orthosilicates, 919 p. Longman Group Limited, New York.

Dobson, D.C. (1982) Geology and alteration of the Lost River tin and tungsten fluorine deposit, Alaska. Economic Geology, 77, 1033–1052.

Dyar, M.D., and Burns, R.G. (1986) Mössbauer spectral study of ferruginous one-layer trioctahedral micas. American Mineralogist, 71, 955–965.

Eby, G.N. (1975) Abundance and distribution of the rare-earth elements and yttrium in the rocks and minerals of the Oka carbonatite complex, Quebec. Geochimica et Cosmochimica Acta, 39, 597–620.

——— (1987) Fission-track geochronology of the Arkansas alkaline province. U.S. Geological Survey Open-File Report 87-287, 14 p.

Erickson, R.L., and Blade, L.V. (1963) Geochemistry and petrology of the alkalic igneous complex at Magnet Cove, Arkansas. U.S. Geological Survey Professional Paper 425, 95 p.

Flohr, M.J.K., and Ross, M. (1985a) Nepheline syenite, quartz syenite and ijolite from the Diamond Jo quarry, Magnet Cove, Arkansas. In R.C. Morris and E.D. Mullen, Eds., Alkalic rocks and carboniferous sandstones, Ouachita Mountains: New perspectives, p. 63–75. Guidebook for GSA Regional Meeting, Fayetteville, Arkansas, April 16–18, 1985.

——— (1985b) Pyroxene zoning trends in mafic nepheline syenite and ijolite, Diamond Jo quarry, Magnet Cove, Arkansas. Geological Society of America Abstracts with Programs, 17, 584.

——— (1987) Geochemical trends of and relationships between alkaline rocks from the Magnet Cove igneous complex, Arkansas. Geological Society of America Abstracts with Programs, 19, 664.

Forman, D.W. (1968) Neutron and X-ray diffraction study of $Ca_3Al_2(D_4O_4)_3$, a garnetoid. Journal of Chemical Physics, 48, 3037–3041.

Gerasimovsky, V.I. (1974) Trace elements in selected groups of alkaline rocks. In H. Sørensen, Ed., The alkaline rocks, p. 402–412. Wiley, New York.

Gerasimovsky, V.I., Volkov, V.P., Kogarko, L.N., Polyakov, A.I., Saprykina, T.V., and Balashov, Yu.A. (1968) The geochemistry of the Lovozero alkaline massif, Part 2, Geochemistry, 369 p. Australian National University Press, Canberra (translated from Geochemistry of the Lovozero Alkaline Massif, Nauka, Moscow, 1966).

Gunow, A.J., Ludington, S., and Munoz, J.L. (1980) Fluorine in micas from the Henderson molybdenite deposit, Colorado. Economic Geology, 75, 1127–1137.

Hamilton, D.L. (1961) Nephelines as crystallization temperature indicators. Journal of Geology, 69, 321–329.

Higgins, J.B., and Ribbe, P.H. (1976) The crystal chemistry and space groups of natural and synthetic titanites. American Mineralogist, 61, 878–888.

Huggins, F.E., Virgo, D., and Huckenholz, H.G. (1977) Titanium-containing silicate garnets. I. The distribution of Al, Fe^{3+} and Ti^{4+} between octahedral and tetrahedral sites. American Mineralogist, 62, 475–490.

Kogarko, L.N. (1974) The role of volatiles. In H. Sørensen, Ed., The alkaline rocks, p. 474–487. Wiley, New York.

Le Bas, M.J. (1977) Carbonatite-nephelinite volcanism, 347 p., Wiley, New York.

——— (1981) Carbonatite magmas. Mineralogical Magazine, 44, 133–140.

Madel, R.E., Smyth, J.R., McCormick, T.C., and Munoz, J.L. (1987) A crystal structure refinement of a fluorine-bearing garnet (abs.). EOS, 68, 1539.

McGee, J.J. (1983) $ANBA—A rapid, combined data acquisition and correction program for the SEMQ electron microprobe. U.S. Geological Survey Open-File Report 83-817, 45 p.

——— (1985) ARL-SEMQ electron microprobe operating manual. U.S. Geological Survey Open-File Report 85-387, 62 p.

Mitchell, R.H., and Brunfelt, A.O. (1975) Rare earth element geochemistry of the Fen alkaline complex, Norway. Contributions to Mineralogy and Petrology, 52, 247–259.

Morimoto, N. (1988) Nomenclature of pyroxenes. American Mineralogist, 73, 1123–1133.

Morris, E.M. (1987) The Cretaceous Arkansas alkalic province: A summary of petrology and geochemistry. Geological Society of America Special Paper 215, 217–233.

Munoz, J.L. (1984) F-OH and Cl-OH exchange in micas with applications to hydrothermal ore deposits. Mineralogical Society of America Reviews in Mineralogy, 13, 469–493.

Nash, W.P., and Wilkinson, J.F.G. (1970) Shonkin Sag laccolith, Montana, I. Mafic minerals and estimates of temperature, pressure, oxygen fugacity, and silica activity. Contributions to Mineralogy and Petrology, 25, 241–269.

Nelson, D.R., Chivas, A.R., Chappell, B.W., and McCulloch, M.T. (1988) Geochemical and isotopic systematics in carbonatites and implications for the evolution of ocean-island sources. Geochimica et Cosmochimica Acta, 52, 1–17.

Owens, D.R., and Howard, J.M. (1989) Bedrock mapping and geology of the Diamond Jo quarry. Arkansas Geological Commission Open-File Report, in press.

Rinaldi, R., and Wenk, H.-R. (1979) Stacking variations in cancrinite minerals. Acta Crystallographica, A35, 825–828.

Ross, M. (1984) Ultra-alkalic arfvedsonite and associated richterite, acmite, and aegerine-augite in quartz syenite, Magnet Cove igneous complex, Arkansas (abs.). EOS, 65, 293.

Sage, R.P. (1987) Geology of carbonatite–alkalic rock complexes in Ontario: Prairie Lake Carbonatite Complex, District of Thunder Bay. Ontario Geological Survey, Study 46, 91 p.

Schnetzler, C.C., and Philpotts, J.A. (1970) Partition coefficients of rare-earth elements between igneous matrix material and rock-forming mineral phenocrysts—II. Geochimica et Cosmochimica Acta, 34, 331–340.

Sørensen, H. (1974) The alkaline rocks, 622 p. Wiley, New York.

Spear, J.A. (1984) Micas in igneous rocks. Mineralogical Society of America Reviews in Mineralogy, 13, 299–356.

Tilley, C.E. (1954) Nepheline-alkali feldspar parageneses. American Journal of Science, 252, 65–75.

Valley, J.W., Essene, E.J., and Peacor, D.R. (1983) Fluorine-bearing garnets in Adirondack calc-silicates. American Mineralogist, 68, 444–448.

Van Marcke de Lummen, G. (1986) Fluor-bearing hydro-andradite from an altered basalt in the Land's End area, SW England. Bulletin de Minéralogie, 109, 613–616.

Waychunas, G.A. (1987) Synchrotron radiation XANES spectroscopy of Ti in minerals: Effects of Ti bonding distances, Ti valence, and site geometry on absorption edge structure. American Mineralogist, 72, 89–101.

Weiss, R., and Grandjean, D. (1964) Structure de l'aluminate tricalcique hydrate, $3CaO \cdot Al_2O_3 \cdot 6H_2O$. Acta Crystallographica, 17, 1329–1330.

Williams, J.F. (1891) The igneous rocks of Arkansas. Arkansas Geological Survey Annual Report 1890, 2, 1–391, 429–457.

Yun, S., and Einaudi, T. (1982) Zinc-lead skarns of the Yeonhwa-Ulchin district, South Korea. Economic Geology, 77, 1013–1032.
Zartman, R.E. (1977) Geochronology of some alkalic rock provinces in eastern and central United States. Annual Review of Earth and Planetary Sciences, 5, 257–286.

Manuscript received January 14, 1988
Manuscript accepted September 26, 1988

Appendix 1. Calculation of garnet formulae

Calculation of formulae of F-free garnets

Fe^{3+} was calculated from electron-microprobe analyses (Table 5) by assuming ideal garnet stoichiometry of 8 cations per 12 oxygens. Cation-site occupancies were calculated by using the following procedure. Ti-bearing garnets are silica deficient and have <3 Si per 12 oxygens. Huggins et al. (1977) concluded that the preference for filling the tetrahedral site in such garnets is Al > Fe^{3+} > Ti. Waychunas (1987), in a spectroscopic study of a variety of Ti-rich minerals, found no evidence for significant amounts of Ti^{4+} in tetrahedral coordination in silicates. In view of these observations, the tetrahedral site was filled in the order Si, Al, and Fe^{3+}. The octahedral site was filled with all remaining trivalent and tetravalent cations (Al, Fe^{3+}, V, Ti, Zr) followed by the divalent cations, according to ionic radius, in the order Mg, Fe^{2+}, Mn, and Ca. The dodecahedral site was filled primarily with Ca, any remaining divalent cations, and Na. The need to place Ca in the octahedral site in three of the analyses (Table 5, nos. 6, 7, 8) is puzzling and may reflect analytical error. Ca in excess of 3 cations per 12 oxygens has been reported by other investigators (Huggins et al., 1977; Waychunas, 1987) in Ti-rich garnets in which there appears to be a deficiency in the octahedral site, suggesting that minor amounts of Ca may enter the octahedral site.

Calculation of formulae of fluoro-hydrograndites

The example in Appendix Table 1 illustrates the method for calculating the chemical formula of fluoro-hydrograndite from an electron-microprobe analysis. The analysis used in this example is from Table 6, no. 1 (sample 1-166B).

1. Column A gives the original electron-microprobe analysis with all Fe converted to Fe^{3+}. We assume that the difference between 100% and the oxide sum (adjusted for the F equivalent of oxygen) is equal to the water content.

2. Calculate the initial atomic ratios, the total number of cations (cation sum) and anions (anion sum), and the sum of cationic charges [$\Sigma(+)$], as shown in column B.

3. Derive the factor K for converting the initial atomic ratios into the final atomic ratios by noting that the sum of the cationic charges excluding hydrogen [$\Sigma(+)$] must equal the sum of the anionic charges of oxygen, F, and hydroxyl,

$$\Sigma(+) = 2(O) + F + OH, \quad (1)$$

and that the garnet formula requires that the total number of oxygen, F, and hydroxyl anions be equal to 12,

$$O' + F' + OH' = 12, \quad (2)$$

where primes indicate the final anionic ratios. The K factor is equal to the quotient of the final anionic to the initial anionic ratios (column B),

$$K = (O' + F' + OH')/(O + F + OH) \quad (3)$$

Appendix Table 1. Calculation of the chemical formula of fluoro-hydrograndite

	A		B	C
SiO_2	31.7	Si	0.5276	2.471
TiO_2	2.47	Ti	0.0309	0.145
ZrO_2	0.09	Zr	0.0007	0.003
Al_2O_3	10.9	Al	0.2139	1.002
V_2O_3	0.44	V	0.0059	0.028
Fe_2O_3	13.9	Fe^{3+}	0.1741	0.815
MnO	0.08	Mn	0.0011	0.005
MgO	0.19	Mg	0.0047	0.022
CaO	36.3	Ca	0.6473	3.032
Na_2O	0.04	Na	0.0013	0.006
F	2.94			
Sum	99.05	Cation sum	1.6075	7.529
$-F \equiv O$	−1.24	$\Sigma(+)$	4.7259	22.135
		F	0.1547	0.725
Sum	97.81	OH	0.2431	1.139
H_2O	2.19	O	2.1641	10.136
Sum	100.00	Anion sum	2.5619	12.000
		$\Sigma(-)$	4.7260	22.136
K factor			4.6841	

and by Equation 2,

$$K = 12/(O + F + OH). \quad (4)$$

Solving Equation 1 for oxygen (O) and substituting in Equation 4, we have

$$K = 24/(\Sigma(+) + F + OH). \quad (5)$$

4. Calculate the final atomic ratios (column C) by multiplying column B values by K.

5. In the fluoro-hydrograndite crystal structure, some SiO_4^{4-} groups are replaced by F_4^{4-} and $(OH)_4^{4-}$ groups, i.e., $A_3B_2(SiO_4)_{3-x}(F,OH)_{4x}$ where A and B occupy the dodecahedral and octahedral sites, respectively. Each Si vacancy is thus represented by F/4 or OH/4 as indicated in Table 6.

6. Cations and tetrahedral vacancies can now be allocated to the tetrahedral, octahedral, and dodecahedral sites as given in Table 6. The tetrahedral site is filled in the order Si, vacancies (expressed as F/4 and OH/4 in Table 6), and, last, Al to give a sum of 3.000. The octahedral site is filled with the remaining Al, then Ti, Zr, V^{3+}, Fe^{3+}, and then the divalent ions Mn and Mg. In all our analyses of fluoro-hydrograndites, the octahedral site is slightly deficient in total cations after allocation of Mn and Mg while the dodecahedral site contains some excess Ca. The dodecahedral site is filled with Na and then Ca to give a total of 3.000; the excess Ca is assigned to the octahedral site. The total number of cations plus the tetrahedral vacancies (shown as F/4 and OH/4 in Table 6) in our analyses is close to 8.000.

Calculation of hydrogarnet and fluoro-hydrogarnet chemical formulas by summing to 8.000 cations (filled tetrahedral, octahedral, and dodecahedral sites) is not valid for the tetrahedral sites containing vacancies. Summation to 5.000 cations (filled octahedral and dodecahedral sites) or to 3.000 cations (filled dodecahedral sites) can also lead to significant error because Al may occupy both the tetrahedral and octahedral sites and a variety of cations may occupy both the octahedral and dodecahedral sites.